Geochemistry
Geophysics
Geosystems
G3
AN ELECTRONIC JOURNAL OF THE EARTH SCIENCES
Published by AGU and the Geochemical Society

Article
Volume 5, Number 5
13 May 2004
Q05004, doi:10.1029/2003GC000597
ISSN: 1525-2027

Composition of the depleted mantle

Vincent J. M. Salters
National High Magnetic Field Laboratory and Department of Geological Sciences, Florida State University, Tallahassee, FL 32312, USA (salters@magnet.fsu.edu)

Andreas Stracke
Department of Earth Sciences, University of Cambridge, Downing Street, Cambridge CB2 3EQ, UK

Now at Abteilung Geochemie, Max-Planck-Institut für Chemie, J. J. Becher Weg 27, 55128 Mainz, Germany (stracke@mpch-mainz.mpg.de)

[1] We present an estimate for the composition of the depleted mantle (DM), the source for mid-ocean ridge basalts (MORBs). A combination of approaches is required to estimate the major and trace element abundances in DM. Absolute concentrations of few elements can be estimated directly, and the bulk of the estimates is derived using elemental ratios. The isotopic composition of MORB allows calculation of parent-daughter ratios. These estimates form the "backbone" of the abundances of the trace elements that make up the Coryell-Masuda diagram (spider diagram). The remaining elements of the Coryell-Masuda diagram are estimated through the composition of MORB. A third group of estimates is derived from the elemental and isotopic composition of peridotites. The major element composition is obtained by subtraction of a low-degree melt from a bulk silicate Earth (BSE) composition. The continental crust (CC) is thought to be complementary to the DM, and ratios that are chondritic in the CC are expected to also be chondritic in the DM. Thus some of the remaining elements are estimated using the composition of CC and chondrites. Volatile element and noble gas concentrations are estimated using constraints from the composition of MORBs and ocean island basalts (OIBs). Mass balance with BSE, CC, and DM indicates that CC and this estimate of the DM are not complementary reservoirs.

Components: 13,973 words, 9 figures, 8 tables, 2 datasets.

Keywords: mantle geochemistry.

Index Terms: 1010 Geochemistry: Chemical evolution; 1025 Geochemistry: Composition of the mantle; 1040 Geochemistry: Isotopic composition/chemistry.

Received 7 July 2003; **Revised** 30 January 2004; **Accepted** 5 March 2004; **Published** 13 May 2004.

Salters, V. J. M., and A. Stracke (2004), Composition of the depleted mantle, *Geochem. Geophys. Geosyst.*, *5*, Q05004, doi:10.1029/2003GC000597.

1. Introduction

[2] One way to constrain the chemical evolution of the Earth is by determining the composition of its differentiation products. The composition of the atmosphere and the crust can be determined by direct measurement. However, the composition of any of the other reservoirs is dependent on models. This paper provides a new estimate and reasonable uncertainties for the depleted mantle reservoir. The depleted mantle is defined as mantle that can generate MORB which is uncontaminated by enriched or plume components.

[3] Beneath mid ocean ridges basalts are produced by partial melting of the underlying mantle at a

current rate of 21 $km^3\ a^{-1}$; assuming a production rate of 3 $km^2\ a^{-1}$ [*Hofmann and White*, 1982] and an average crustal thickness of 7 km [*White et al.*, 1992]. This can be considered a lower bound if oceanic crust production is controlled by heat production. Assuming oceanic crust production has been constant over the history of the Earth the total amount of oceanic crust (density 3 gr/cm^3) produced equals 8% of Earth's mantle. If we assume further that the oceanic crust represents an average of 10% melt, then roughly the equivalent of 80% of the total volume of the mantle could have been processed at the ridge and would have to be classified as "depleted mantle." This 80% of the total mantle is an upper estimate as mantle processed at the ridge once, can be re-enriched and reprocessed and thus the 80% number is a potential. Nevertheless, considering the potentially large proportion of the depleted mantle relative to the total mantle, or even the entire volume of the Earth, it is obvious that the composition of the DM is a key parameter in understanding the composition and chemical evolution of the Earth.

[4] The DM in our definition is assumed to yield the depleted end of the spectrum of MORB and does not contain a recognizable enriched component. An enriched component is defined as radiogenic Sr-isotopic composition, and unradiogenic Nd, Hf and Pb isotopic composition as well as elevated abundances of large-ion-lithophile elements. MORB ranges in composition from depleted (or normal, N-type) to enriched (E-type), whereby normal MORB are tholeiites from normal ridge segments. Normal ridge segments are originally described as segments with "well developed and symmetrical magnetic anomaly lineaments, typical oceanic crustal thickness and structure, similar and uniform characteristics of subsidence of the lithosphere independent of spreading rate and greater seismicity than transitional ridge segments" [*Schilling*, 1975]. MORB of these ridge segments are tholeiitic, relatively depleted large ion lithophile element abundances chondrite normalized La/Sm < 1 and unradiogenic $^{87}Sr/^{86}Sr$ [*Schilling*, 1975]. However, even N-type MORB displays a range of compositions and the definition of N-type MORB is arbitrary. As MORB are used to estimate a large number of trace elements in DM, care has to be taken to use only those MORB that are representative of DM. Recognizable enriched components are often associated with thermal anomalies, a higher degree of melting and shallow ridge segments. Therefore most ridge basalts erupted at the deeper ridges (in excess of 2000 m) arguably lack an enriched component. However, this filter does not necessarily remove all ridge basalts with an enriched component. As DM has $^{143}Nd/^{144}Nd$ and $^{176}Hf/^{177}Hf$ higher than chondritic and $^{87}Sr/^{86}Sr$ lower than chondritic the reservoir has to have evolved with the appropriate Sm/Nd, Lu/Hf and Rb/Sr ratios. These parent-daughter ratios determine the general trace element characteristics of DM, and MORB that are used to estimate DM should have the appropriate trace element characteristics. We will also use additional chemical criteria to identify "depleted" (i.e., lacking an enriched component) MORB and will show that the choice of criteria influences the final composition of DM.

[5] The evolution and creation of the DM is most likely a continuous process, the DM most likely represents a mixture of materials at different stages in their evolution, and is unlikely to be a compositionally homogeneous reservoir. Several observations show that the source material for MORB is compositionally heterogeneous at different scales in both chemical composition and mineralogy: 1) young near-ridge Pacific Seamounts are chemically and isotopically more variable that the adjacent ridge basalts [*Graham et al.*, 1988; *Zindler et al.*, 1984]; 2) the magnitude of isotopic variability in MORB is dependent on spreading rate [*Batiza*, 1984; *Stracke et al.*, 2003b]; 3) MORB that is arguably not influenced by plume material still shows a range in compositions, 4) the isotopic composition of abyssal peridotites along the southwest Indian Ridge is different from the isotopic composition of related basalts [*Salters and Dick*, 2002], and 5) basalts from Garrett fracture zone (Pacific ocean) and basalts from the Australian-Antarctic Discordance (Indian ocean) have a more depleted isotopic signatures than basalts from adjacent ridge segments and are interpreted to be derived from previously depleted mantle [*Hanan et*

al., 2000; *Wendt et al.*, 1999]. Taking all these observations together, in addition to age variations, the DM is likely to contain a range of potentially enriched components, which are of relatively small mass relative to the total mass of the DM. Therefore any estimate of the composition of the DM should be used with considerable caution and with thorough knowledge of the limitations of such an estimate.

[6] The estimate of the abundance of most elements depends on the concentration of other elements. By detailing how the estimate for the individual elements is derived we also intend to show the inter-relationship between the estimates of the different elements. The attempt is made to provide a, to us, "most reasonable" estimate of DM, but it is realized that it depends on assumptions that might not be viewed as "most reasonable" by all or that some assumptions or criteria might later prove to be wrong. To address these variations as well as to accommodate preconceived notions that are different from ours, we provide a Microsoft Excel™ worksheet (Table A2) with full access to the calculations used to estimate the concentrations of the elements. This enables the reader to use different values and evaluate the consequences of those changes for the concentration of dependent elements.

2. Estimating the Composition of the DM

[7] Since the DM is not directly accessible, its composition has to be inferred via constraints derived from rocks, whose origin and composition are related to the DM (i.e., MORB, peridotites, chondritic meteorites and crustal rocks). Previously, the isotopic composition of MORB has been used to estimate parent-daughter ratios (e.g., Sm/Nd, U/Pb, U/Th) and the respective element concentrations in the DM (e.g., Sm, Nd, U, Pb, etc. [e.g., *Albarède and Brouxel*, 1987; *Elliott et al.*, 1999; *Galer and O'Nions*, 1985]). A larger number of element concentrations has been estimated using the trace element patterns of MORB [*Hofmann*, 1988; *Sun and McDonough*, 1989]. Our new estimate of the composition of the DM uses constraints from both the isotopic and chemical composition of MORB wherever possible. Additional constraints come from the composition of peridotites, chondritic meteorites and the CC. Figure 1 shows how we derive the estimates for the individual elements and the inter-relationship between the estimates of the different elements.

2.1. Strategy to Estimate the Composition of MORB

[8] In the following, the different avenues to estimate element concentrations in the DM are described in order of directness of the relation to the DM. Clearly, the estimate will be more accurate the closer the relation between the source of information and the DM. MORB and peridotites are directly related to the DM by partial melting; MORB are the melting products, peridotites the residue of partial melting. The isotopic composition of MORB directly reflects the isotopic composition of its source, the DM, and is the most reliable constraint on the trace element ratio formed by the parent and daughter element of the isotopic system considered. For example, by measuring ^{143}Nd/^{144}Nd in MORB, the ratio of the parent element Sm and the daughter element Nd (Sm/Nd) can be calculated with some information on the isotopic evolution of the DM. These calculated parent-daughter ratios form the framework for our estimates of other trace element ratios. The Sr, Nd and Pb isotopic composition of average MORB is used to estimate parent-daughter ratios in the DM (the average MORB composition results from compiling MORB from the PetDB database; see below). A depleted isotopic composition for MORB is also used to evaluate what the most suitable isotopic composition of the DM is.

[9] Trace element ratios in basalts that are relatively constant over a large concentration range are another reliable estimate of the trace element composition of the DM. This method was championed by the Mainz group [*Hofmann*, 1986, 1988; *Hofmann et al.*, 1986b; *Jochum et al.*, 1983, 1986, 1991] and is based on the assumption that differences in absolute trace element content reflect variations in the degree of melting and variable degrees of enrichment. The constancy

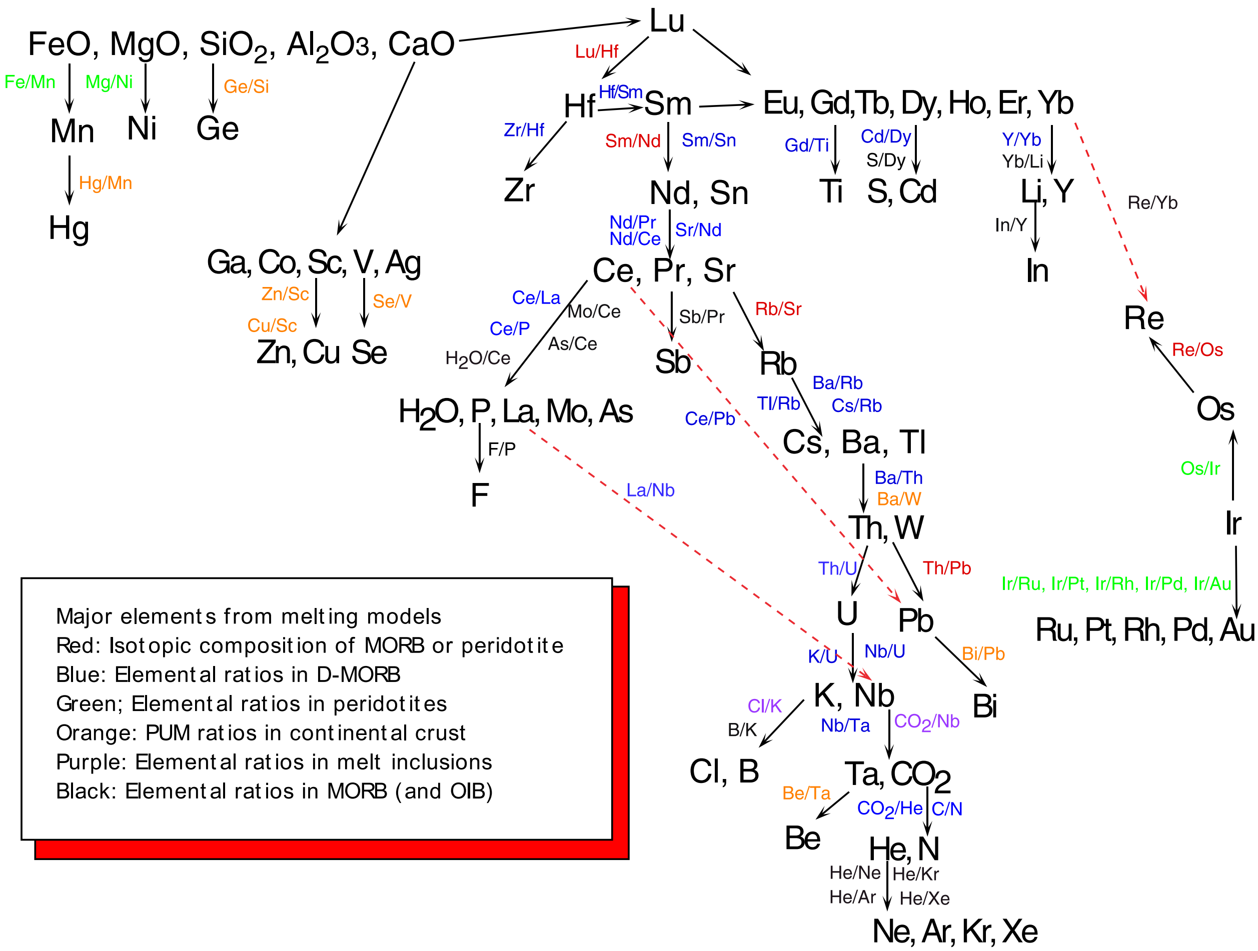

Figure 1. Genealogy of the elements in the DM. Chart showing the dependencies of the concentrations on the trace element ratios.

of a trace element ratio over a range of concentrations indicates that these two elements have similar partitioning behavior during partial melting (and subsequent crystallization). The ratio in the basalt is therefore identical to the ratio in the source, the DM. Especially highly incompatible elements (elements that do not readily fit into the crystal structure of common minerals in the mantle and basalts), have the same trace element ratio in the basalt as in their source (DM), because these elements are quantitatively removed from their source after only a few percent of melting. The combination of the isotopes and the constant ratios allow us to calculate the trace element ratios of most elements on the Coryell-Masudo diagram.

[10] The chemical compositions of peridotites provide a third constraint. Compatible trace elements are effectively retained in the source during melting and residues of melting such as abyssal peridotites should provide accurate estimates of the compatible trace element concentrations of DM. Furthermore, the chemical variations in anhydrous peridotites are, in general, thought to be related to variations in degree of depletion, i.e., degree of melting [*Hart and Zindler*, 1986; *Jagoutz et al.*, 1979; *Sun*, 1982]. The major element composition of the DM can be estimated from melting experiments, by subtracting a low degree melt from a bulk Earth composition. This estimate for the major element composition of the DM can also be used to constrain elemental concentrations of trace elements that show correlations with major elements in peridotites.

[11] Another possible and perhaps least reliable estimate can be derived from the composition of the chondritic meteorites and CC. It is generally

assumed that the Earth initially had a chondritic composition. During differentiation of the Earth, distribution of the elements is dependent on their chemical behavior, so that different elements are distributed unevenly between the discrete reservoirs. Thus if two elements maintain a chondritic ratio in the CC their relative distribution is likely to be unaffected by differentiation of the Earth. In the absence of any other data, a first order estimate can be made by assuming that a trace element ratio that is chondritic in the crust is also chondritic in the DM. Trace elements ratios that include an element with known concentration can thus be used to calculate the concentration of the unknowns.

2.2. Estimating Parent-Daughter Ratios

[12] With some information about the average isotopic evolution of the DM, the present-day isotopic composition of MORB can be used to calculate the parent-daughter ratios in the DM. Previously two stage models have been used to estimate the age and parent-daughter ratio of the MORB source. However, for the U-Th-Pb system it has been shown that a simple two-stage evolution cannot explain both the observed U-Th-Pb concentrations and the Th-Pb isotopic compositions of the basalts [*Elliott et al.*, 1999; *Galer and O'Nions*, 1985]. One possibility is that the DM is an open system whereby U, Th and Pb have different exchange rates, and therefore have different residence times in non-DM mantle and CC [*Galer et al.*, 1989; *Galer and O'Nions*, 1985; *Paul et al.*, 2002]. A second class of models argues that the discrepancy between the long-term and recent U-Th-Pb ratios is related to the change in recycling behavior of U when the atmosphere changed from oxygen-poor to oxygen-rich [*Elliott et al.*, 1999]. Assuming that the major processes leading to differentiation of the Earth are crust formation and subduction, it is easy to envisage a difference in behavior in U related to the formation of an oxygen-rich atmosphere.

[13] Although the DM might be, and most likely is, an open system a simple two-stage model with a chondritic evolution during the first part and subsequent evolution to present-day average parent-daughter ratios is expected to agree well with the actual average parent-daughter ratio of the DM. The age of this single depletion event is an average age of the depletion of the DM; actual formation of the reservoir is not related to a single event, but is expected to be continuous. Using this approach it is assumed that processes operating on the mantle resulting in chemical change and formation of the DM reservoir have been constant through time. This assumption is reasonable for the Rb-Sr, Sm-Nd, and Lu-Hf isotopic system. The same holds true for the Th-Pb system, with the exception of the early part of Earth's history may have been lost to the core (first 20 Ma [*Kleine et al.*, 2002; *Yin et al.*, 2002]) or lost due its relatively high volatility. The open-system and U recycling model both predict constant Th/Pb ratios in the DM [*Elliott et al.*, 1999; *Galer et al.*, 1989; *Galer and O'Nions*, 1985]. We therefore do not use parent-daughter ratios involving U, e.g., U/Pb for our estimate.

[14] Here we estimate Th/Pb, Lu/Hf, Sm/Nd, and Rb/Sr ratios from the isotope systems assuming a single depletion event for the formation of DM, i.e., a two-stage growth history with a BSE evolution during the first stage and subsequent evolution of the DM to its present-day isotopic composition. The composition of BSE has been estimated by McDonough and Sun [*McDonough and Sun*, 1995]. For the BSE ^{176}Hf/^{177}Hf we use the average for C-chondrites [*Patchett et al.*, 2004] as this results in a BSE composition that falls within the Hf-Nd array on an isotope correlation diagram. In the calculation we also use the recently determined half-life for ^{176}Lu which is lower than earlier determinations [*Scherer et al.*, 2001; *Söderlund et al.*, 2004].

[15] To achieve an average isotopic composition of the DM, we used the PetDB database (http://petdb.ldeo.columbia.edu/petdb/query.asp). We compiled all eruptive products from mid-ocean spreading centers and filtered the data to include only samples that were erupted in water depths in excess of 2000 m and excluded samples that had more than 55 wt.% SiO_2. If REE patterns were available we excluded samples with non-smooth REE patterns. Using this minimum amount of filtering at least part of the plume influenced

Table 1. Isotopic Compositions of DM

	$^{143}Nd/^{144}Nd$	$^{176}Hf/^{177}Hf$	$^{87}Sr/^{86}Sr$	$^{208}Pb/^{204}Pb$
BSE	0.512634	0.282843	0.7045	17.7
Average D-MORB	0.51311	0.2833	0.7026	37.92
Extreme D-MORB	0.5134	0.2836	0.7020	37.2
All MORB	0.5131	0.28328	0.7027	37.9

basalts are excluded. This compilation is called the "All-MORB" data set. The isotopic compositions at the most depleted end of the MORB field are also used and are referred to as "extreme" isotopic compositions. These isotopic compositions are very similar to the average and extreme isotopic compositions obtained by using the compilation of MORB from *Stracke et al.* [2003a]. Table 1 lists the isotopic composition using "average" and "extreme" choices for the present-day MORB. We also used a more restrictive set of filters in order to assure that MORB representing low degree melts or melts which have experienced large amounts of fractional crystallization do not affect the average. Although degree of melting or fractional crystallization does not effect the average isotopic composition, for incompatible trace element ratios to reflect source compositions only high degree melts should be used. The rationale and type of filters is explained in detail in the next section. We will call this compilation "D-MORB." It should be noted however that the isotopic composition of the two averages is very similar.

[16] Tables 2a and 2b list calculated parent-daughter ratios using the average and extreme isotopic composition of the DM for the range of ages for the depletion event of the two-stage evolution model. A minimum depletion age of 1.8 Ga age was used, which is similar to the minimum age expected from the Pb-isotope systematics in MORB (1.8 Ga [*Hart*, 1984; *Tatsumoto*, 1978]). We have limited our calculations to a maximum depletion age of 3.4 Ga inferred from the Re-Os isotope systematics (see below). Estimates for the average age of the CC are approximately 2.2 Ga [*Chase and Patchett*, 1988; *Condie*, 2000; *Galer et al.*, 1989] and if the DM is assumed to be complementary to the CC a similar average age is expected.

[17] Varying the average age of the DM (between 1.8 and 3.4 Ga) results in a 14% and 20% variation in potentially viable Sm/Nd and Lu/Hf ratios respectively, and an even larger potential range for Rb/Sr. The large potential range in Rb/Sr ratio is partly the result of our poor understanding of the Sr-isotope evolution of Earth. The $^{87}Sr/^{86}Sr$ of bulk silicate Earth (BSE) is poorly known, between 0.7040 and 0.7055 if estimated from the Nd-Sr-isotope correlation in oceanic volcanics [*Zindler and Hart*, 1986]. With a Rb/Sr ratio of BSE 0.029–0.030 [*Hofmann and White*, 1983; *McDonough and Sun*, 1995] and initial $^{87}Sr/^{86}Sr = 0.69898$ [*Allègre et al.*, 1975] $^{87}Sr/^{86}Sr$ for BSE is between 0.7046 and 0.7045. With these values the BSE growth curve reaches present-day MORB $^{87}Sr/^{86}Sr$

Table 2a. Key Trace Element Ratio Variations as Function of the Age of DM Using All-MORB Data Set With La < 5 ppm

P/D[a]	1.8 Ga	2.2 Ga	2.8 Ga	3.4 Ga	2.2 GaE[b]	2.8 GaE[b]	3.4 GaE[b]
Rb/Sr	0.0058	0.0103	0.0146	0.0174	0.0022	0.0083	0.0123
Sm/Nd	0.3892	0.3774	0.3661	0.3587	0.4006	0.3842	0.3736
Lu/Hf	0.3303	0.3138	0.2979	0.2876	0.3682	0.3404	0.3224
Th/Pb	0.6170	0.6005	0.5845	0.5742	0.5057	0.5112	0.5147
La/Nb	3.0	1.7	1.2	1.0	7.6	2.1	1.4
Ce/Pb	78.5	43	29.4	24.2	165	45.1	30.9

[a] P/D ratio of elemental concentrations for element (P) that contains the radioactive parent isotope and element (D) concentration with radiogenic daughter isotope.

[b] E stands for extreme isotopic composition for DM (see Table 1).

Table 2b. Key Trace Element Ratio Variations as Function of the Age of DM Using D-MORB Data Set

P/D[a]	1.8 Ga	2.2 Ga	2.8 Ga	3.4 Ga	2.2 GaE[b]	2.8 GaE[b]	3.4 GaE[b]
Rb/Sr	0.0042	0.0089	0.0136	0.0165	0.0022	0.0083	0.0123
Sm/Nd	0.3911	0.3789	0.3672	0.3596	0.4006	0.3842	0.3736
Lu/Hf	0.3352	0.3178	0.3010	0.2902	0.3682	0.3404	0.3224
Th/Pb	0.6080	0.5932	0.5789	0.5697	0.5057	0.5112	0.5147
La/Nb	2.4	1.1	0.7	0.6	4.4	1.2	0.8
Ce/Pb	74	33.4	21.5	17.3	113.1	30.9	21.1

[a] P/D ratio of elemental concentrations for element (P) that contains the radioactive parent isotope and element (D) concentration with radiogenic daughter isotope.

[b] E stands for extreme isotopic composition for DM (see Table 1).

values (0.7027) at 1.8 Ga and at 2.1 Ga using a $^{87}Sr/^{86}Sr$ of present-day MORB of 0.702. Thus these are strong constrains on the minimum age of the DM.

2.3. Trace Element Constraints From MORB

[18] Absolute concentrations are hard to constrain as those depend on the amount of the mantle that is assumed to be depleted. Estimates on the amount of DM range from 10 to 90% [*Allègre et al.*, 1983a, 1983b; *Hofmann*, 1997; *Zindler and Hart*, 1986], which allows for a wide range of possible concentrations. Trace element ratios are better constrained, especially those ratios in basalts that are relatively constant over a large concentration range (i.e., large range in degree of melting) [*Hofmann*, 1986, 1988; *Hofmann et al.*, 1986b; *Jochum et al.*, 1983, 1986, 1991]. This method works best for highly incompatible elements ratios (e.g., Cs/Rb, Ba/Th), which are very similar to the source ratio, while the ratios for the somewhat less incompatible elements like Lu and Sm are likely to be slightly different in the source and the basalts [*Salters*, 1996; *Salters and Hart*, 1989]. Therefore it is important to combine the trace element ratios inferred from the average MORB composition with the parent-daughter ratios estimated from the previous section. In addition, the strong LREE depletion in abyssal peridotites and their low Ce/Nd and La/Ce ratios compared to MORB [*Johnson and Dick*, 1992; *Johnson et al.*, 1990] indicate that the LREE ratios in low-degree melts do not necessarily reflect source compositions. Figure 2 shows that some ratios including similarly compatible elements show some correlated variation with trace element concentration and are only relatively "constant." As these variations can be related to degree of melting for the group of elements with compatibilities between Nd and K a data filter is required to remove low-degree melts from the data set.

[19] To remove low degree melts from the MORB compilation, we tried two different approaches. In the first approach we applied stringent additional filters to select the depleted and high degree melts only: -MgO-content is more than 8 weight percent, -$(La/Sm)_N < 1$, and -$(Sm/Nd)_N > 1$. We then screened this subset and rejected samples that did not have a complete REE pattern (at least 6 REE). Furthermore, we rejected samples with a non-smooth REE patterns. Only a total of 232 samples passed the tests. The data, including locations and references are provided in the accompanying Microsoft^{TM} Excel worksheet (Table A1) and will be called the depleted (D-)MORB data set. The worksheet also reports the standard deviation on the average as well as median, minimum and maximum values. Figure 3 shows the geographic coverage of these samples along the mid-ocean ridges. Inspection of the data set reveals that a large number (94) of samples are from the Mid-Atlantic Ridge between 40° and 50°S. In order to avoid the D-MORB average to be biased by this relatively uniform data set we have averaged each ridge segment and use only the eight averages (6%) in the calculation of the depleted MORB average. A second approach taken was to use the "All-MORB" data set and first remove outliers. Outliers in the data set are identified by calculating the upper and lower quartile range, Q1 and Q3, and by applying the outlier criterion $Q1 - 1.5 * (Q3 - Q1)$ and $Q3 + 1.5 * (Q3 - Q1)$). In addition,

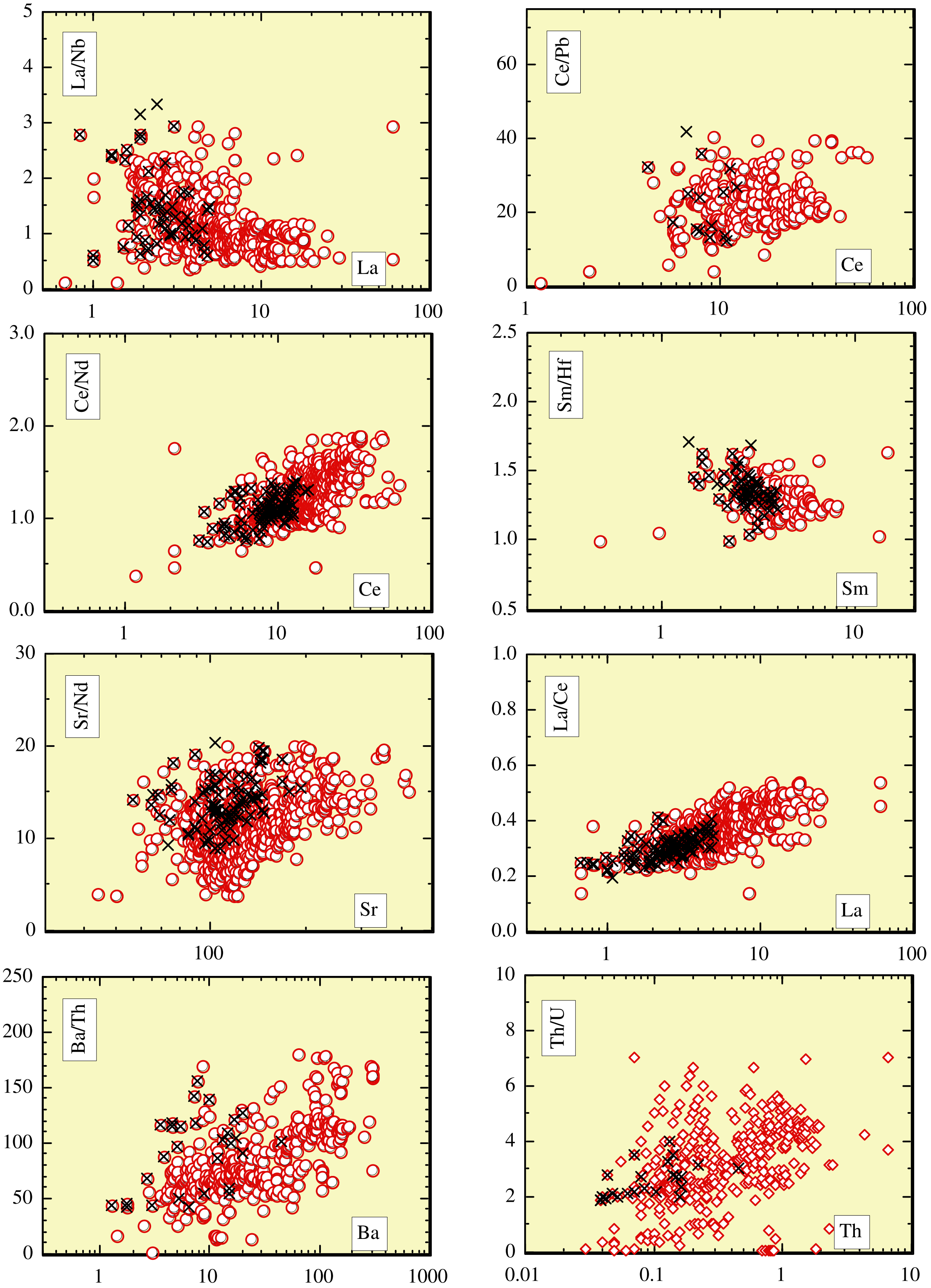

Figure 2. Some of the constant ratios used for the estimate of DM. Crosses are D-MORB compilation; circles are All-MORB compilation. D-MORB ratios show less variation, and correlations with concentrations are less obvious than for All-MORB data.

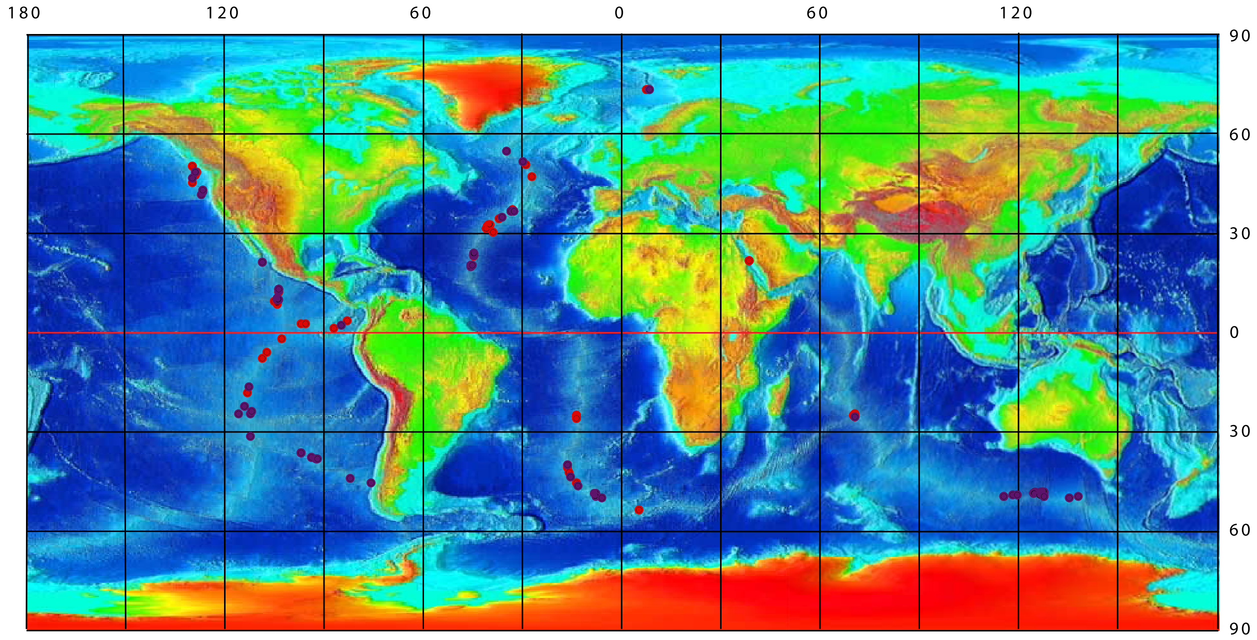

Figure 3. Sample locations of N-type MORB used to make an average composition. Purple circles are glass data; red circles are whole rock.

samples with La > 5 ppm were rejected. This data set contains 639 samples; almost 5 times the number of samples of the D-MORB compilation. Figure 2 compares several of the "constant" ratios for least and most restrictive filtering and shows that the two approaches of removing low degree melts results in very similar ratios, but that significantly different ratios result using the "All-MORB" compilation. Table 3 lists the ratios using the various compilations.

[20] We have chosen the Lu concentration as the "anchoring point" of the trace element pattern. The Lu concentration will be derived in section 2.5. With the Lu concentration as a starting concentration, we use the Lu/Hf ratio derived from the Hf-isotope systematics (see Table 1) and average Sm/Hf of MORB to define Sm/Lu and to estimate the Sm and Hf concentrations. All REE between Lu and Sm were determined using linear interpolation based on atomic number. Thus the slope of the heavy REE pattern is determined by the Hf-isotopic composition. Ti, Zr and Y are determined using the constant Gd/Ti, Hf/Zr and Y/Yb ratios of the compiled D-MORB average (Table 3). Nd was determined using the Sm/Nd derived from the Nd-isotopic composition (see Table 1); Pr, Ce and La were determined using the Nd/Pr, Nd/Ce and Ce/La ratios of compiled D-MORB. Sr was determined using the average Sr/Nd of compiled D-MORB (Table 3), Rb/Sr was derived from the Sr-isotopic composition (see Table 1) and Ba and Th were determined using the Ba/Rb and Ba/Th ratios of compiled D-MORB (Table 3). Th/U = 2.9 was chosen on the basis of the isotope systematics [*Elliott et al.*, 1999; *Galer et al.*, 1989]. This value for Th/U is slightly higher than estimated by *Turcotte et al.* [2001] when mass balancing the CC against the depleted mantle, somewhat lower than our compilations but close to the average obtained using just isotope dilution data. Pb was determined using the Th/Pb ratio from the Th-Pb isotope systematics (see Table 1). Estimates for Cs, K, Nb and Ta were made using Cs/Rb, K/U, Nb/U and Ta/Nb of compiled D-MORB (Table 3). The resulting trace element pattern is shown in Figure 4. Lastly, P_2O_5, arguably a major element is estimated using the constant Ce/P ratio of 0.019 (Tables 2a and 2b). Thus all elements that are commonly used to create a spider diagram are estimated based solely on estimates of the parent-daughter ratios in DM and relatively constant trace element ratios in D-MORB.

Table 3. "Constant" Ratios in MORB

	D-MORB	All-MORB	MORB[a] La < 5
K/U	12654	14674	14319
Ti/Gd	2020	1937	1879
Sr/Nd	13.74	11.88	12.25
Y/Yb	10.144	10.07	9.99
Zr/Hf	39.83	39.03	38.52
Nb/U	44.4	45.74	45.15
Cs/Rb	*0.015*	0.015	0.015
Rb/Ba	0.0731	0.0874	0.0837
La/Ce	0.3026	0.3565	0.3196
Ce/Nd	1.083	1.21	1.09
Nd/Pr	5.443	5.13	5.45
Sm/Hf	1.355	1.32	1.33
Nb/Ta	15.19	14.73	14.19
Ba/Th	87.3	86.04	71.78
Th/U	2.9	3.26	3.04
La/Nb	1.1	1.20	1.396
Ce/Pb	25	22.36	21.55
Ce/P	0.19	0.19	0.19

[a] Only those MORB from the All-MORB data set that have La < 5 ppm.

[21] The above estimate does not "use" the La/Nb and Ce/Pb ratios in MORB, although these ratios are relatively constant despite a large range in concentrations. Therefore these ratios can be used as an independent "check" of the estimate. Nb can be estimated directly from La/Nb in average MORB or, as done here, through the Rb/Sr ratio (which uses the Sr-isotopic composition) followed by Rb/Ba, Ba/Th, Th/U and U/Nb in D-MORB (Figure 1). The Pb estimate can be directly derived from Ce/Pb in D-MORB, or similar to Nb, through Rb/Sr-ratio derived from the Sr-isotopic composition and Rb/Ba, Ba/Th ratios from D-MORB and finally the Th/Pb ratio from the Pb-isotopic composition (Figure 1). Our estimate of Pb and Nb involve two parent-daughter ratios, whose values are dependent on the average age of DM. By adjusting the age and isotopic composition of the DM the Nb and Pb estimate derived using the isotopic composition needs to coincide with the average Ce/Pb and La/Nb obtained from D-MORB. Average Ce/Pb in D-MORB is 22.5 with a 90% of the data between 15 and 42; average La/Nb equals 1.24 with 90% of the data between 0.5 and 3.3. With the Ce/Pb and La/Nb constrains we can put some constrains on the depletion age. With the D-MORB compilation the possible range is 2.0–2.5 Ga, and 2.6–3.2 Ga for average and extreme isotopic compositions respectively. For the large data set (MORB La < 5) the age ranges are similar for average and extreme isotopic compositions (2.0–2.6 Ga and 2.6–3.4 Ga, respectively).

[22] Both the Nb and Pb estimate is obtained through the Rb/Sr ratio (Figure 1) and the calculated depletion age is strongly depend on the preferred Sr-isotope evolution, especially for young depletion ages. If the BSE value for $^{87}Sr/^{86}Sr$ is lowered to 0.7040 the depletion age for DM needs to be reduced by about 400 Ma to keep the Rb/Sr (and Ce/Pb and La/Nb) constant. An average depletion age for DM of 1.8 Ga [*Hart*, 1984; *Tatsumoto et al.*, 1984] is often viewed as the minimum age and this minimum age also constrains the minimum value for $^{87}Sr/^{86}Sr$ of BSE at 0.7045. For our DM estimate we have used the D-MORB compilation and average isotopic composition and the 2.2 Ga depletion age as this is the middle of the possible age range calculated. In the following discussion section we will further justify this choice. The study of *Elliott et al.* [1999] resulted in average ages for the DM that are between 2 and 2.4 Ga. Our 2.2 Ga depletion age is similar to the mean age of the CC [*Condie*, 2000; *DePaolo*, 1980; *McCulloch and Bennett*, 1994].

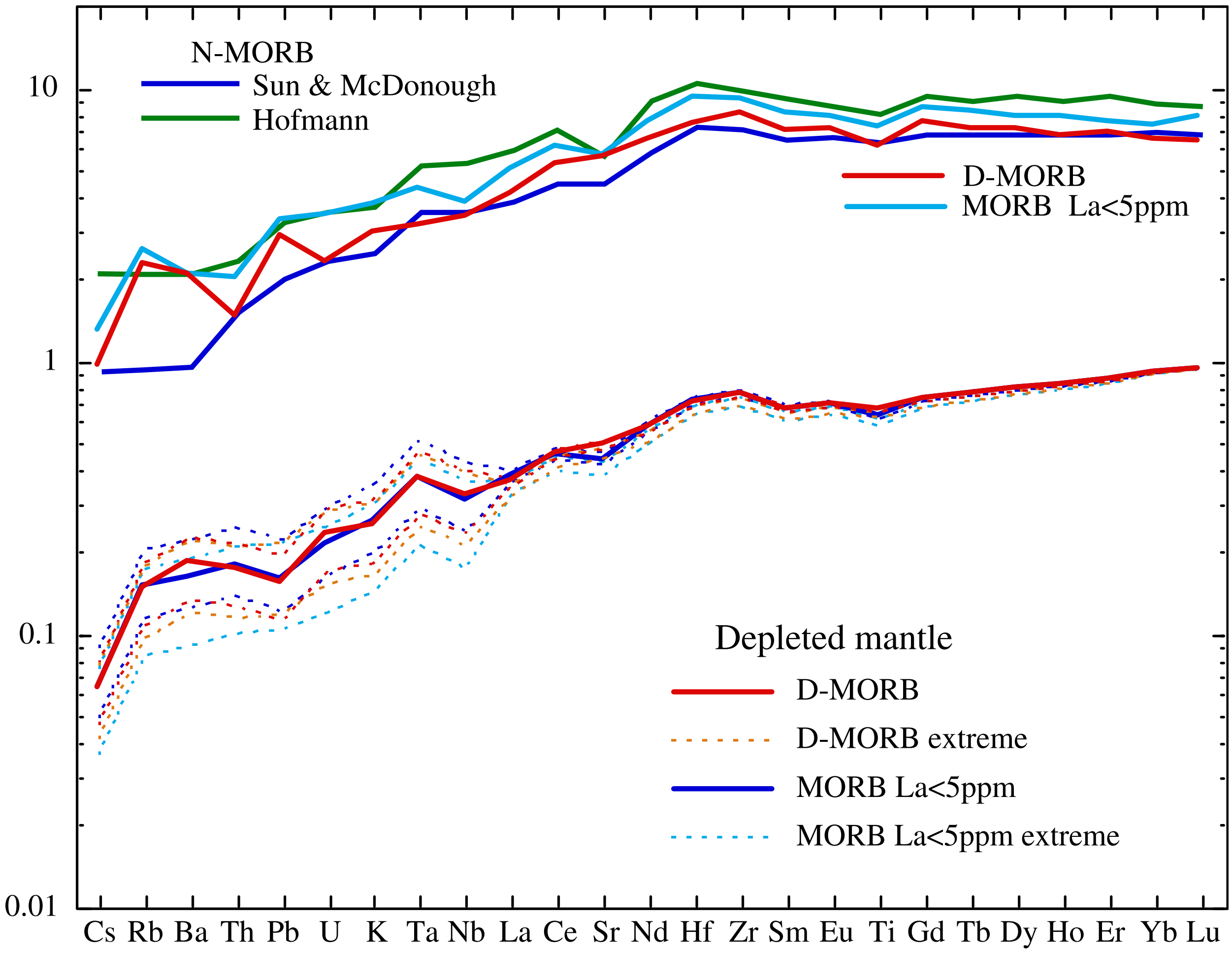

Figure 4. Spider diagram for potential DM composition as well as the average composition of D-MORB and All-MORB that have less than 5 ppm La. DM compositions: red and orange are for D-MORB, blue patterns are for All-MORB that have less than 5 ppm La. Solid lines for DM are for 2.2 Ga depletion age; red and orange patterns are calculated using average and extreme isotopic composition (D-MORB), respectively (see Table 1). The pattern with the shallowest slope represents the DM with the maximum age (given its isotopic composition), and the pattern with the steepest slope represents the minimum age for that isotopic composition. Dark blue patterns represent average isotopic compositions for "All-MORB"; light blue patterns are calculated using extreme "All-MORB." MORB patterns: N-MORB estimates of *Sun and McDonough* [1989] and *Hofmann* [1988] are shown in blue and green, respectively. The pattern for D-MORB is in red, and the pattern for average "All-MORB" with less than 5 ppm La is in light blue. All abundances are normalized to BSE [*McDonough and Sun*, 1995].

[23] Additional complications arise from chemical differences between ocean basins [*Christie et al.*, 1998; *Dupré and Allègre*, 1983; *Klein et al.*, 1988; *White*, 1993], which makes the "average" a more difficult concept. The compiled data from the worksheet show a small difference in Th/U from the Atlantic versus the Pacific Ocean basin. This difference becomes more obvious by considering high quality U-Th isotope dilution data only (see Figure 5). The data in Figure 5 have been screened for hot spot influence. The Th/U of the Pacific ocean basin (sections of the East Pacific Rise and Juan da Fuca Ridge) show, on average, lower Th/U than the Atlantic samples; average Th/U for the Atlantic basin equals 2.92, while the Pacific basin average equals 2.62 [see also *Stracke et al.*, 2003c]. Although little data is available and some is unpublished, the Th/U of the Indian Ocean basin is even higher. The compiled data of primitive MORB results in an average of 2.9, which we chose for our estimate.

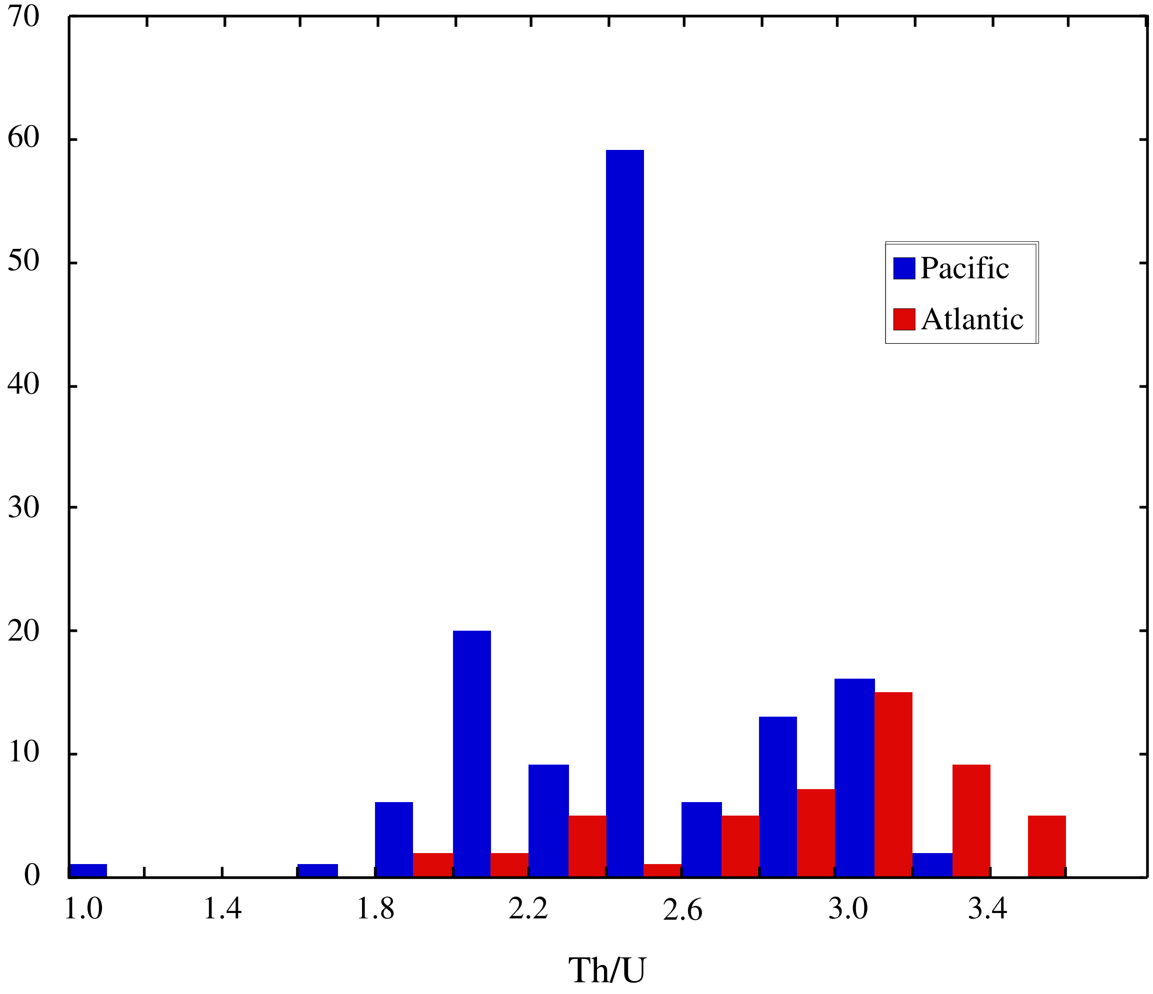

Figure 5. Th/U for the different ocean basins. Data are from *Bourdon et al.* [1993, 1996], *Condomines et al.* [1981], *Goldstein et al.* [1989, 1991, 1993, 1994], *Lundstrom et al.* [1998a, 1998b, 1999], and *Sims et al.* [2002]. Only isotope dilution analyses were used.

[24] For similar depletion ages, but using the different MORB compilations, the calculated range of trace element content in the DM is small. Also, the differences in trace element content of DM due to using different isotopic compositions are limited as they are "damped" by concomitant variations in depletion age differences. A larger uncertainty in the DM compositions is the range in permitted La/Nb and Ce/Pb (see Figure 4). For our preferred estimate of DM (Table 5) we have chosen to use the 2.2 Ga estimate and the average isotopic composition. The trace element ratios of MORB used to calculate the concentrations are based on averages observed in D-MORB and not based on the most extreme composition observed in MORB. Using the average isotopic composition for those basalts thus seems to be more appropriate.

2.4. Concentration Estimates From MORB and OIB Combined

[25] Some elements are poorly defined in MORB alone, but robust estimates can be obtained using constant ratios in MORB and OIB. Although the data set is not as extensive as the one used to obtain the D-MORB estimate the constancy of several trace element ratios over a large compositional range in both MORB and OIB indicates that these ratios are good first order estimates. In/Y = 0.003 and Cd/Dy = 0.027 can be derived from variations in MORB [*Yi et al.*, 2000], as well as Yb/Li =

Table 4. Major Element Composition of DM[a]

		Melt Compositions		DM Compositions					
	BSE	3 GPa	1 GPa	−1% 3 GPa	−1% 1 GPa	−1.5% 3 GPa	−1.5% 1 GPa	1% Mixed	**1.5% Mixed**
SiO_2	45.00	46.18	57.53	44.99	44.87	44.98	44.81	44.93	**44.90**
TiO_2	0.20	1.45	0.59	0.19	0.20	0.18	0.20	0.19	**0.19**
Al_2O_3	4.45	15.29	16.28	4.34	4.33	4.28	4.27	4.34	**4.28**
FeO	8.05	9.72	4.10	8.03	8.09	8.02	8.11	8.06	**8.07**
MgO	37.8	15.49	5.27	38.03	38.13	38.14	38.30	38.08	**38.22**
CaO	3.55	7.00	6.99	3.52	3.52	3.50	3.50	3.52	**3.50**
Na_2O	0.36	2.71	6.87	0.34	0.29	0.32	0.26	0.32	**0.29**
K_2O	0.029	2.16	2.37	0.01	0.01	0.00	0.00	0.01	**0.00**

[a] BSE composition after *McDonough and Sun* [1995]. DM compositions derived by subtraction of 1.0 − 1.5% 3 GPa or 1 GPa melt.

0.55−0.6 [*Ryan and Langmuir*, 1987], B/K = 0.001 [*Ryan and Langmuir*, 1993]. N-MORB have Mo/Ce = 0.034 ± 0.001 [*Sun et al.*, 2003]. This value is in agreement with Mo/Ce = 0.32 of *Sims et al.* [1990] and 0.33 of *Newsom et al.* [1986] based on MORB and OIB.

[26] The amount of data for the chalcophile elements in MORB or peridotite is sparse. However, the small amount of data for MORB can be combined with OIB data and again we can use constant ratios to estimate their concentrations. Sb can be estimated from Sb/Pr = 0.02 (±0.007) [*Jochum and Hofmann*, 1997] or Sb/Ce = 0.0012 (±0.0005) [*Sims et al.*, 1990]. The Jochum and Hofmann estimate is three times higher than the Sims et al one, but this latest estimate is preferred as it is based on an approximately four times larger data set. If the MORB and OIB data are combined one can also obtain As/Ce of 0.0096 (±0.0027), and W/Ba = 0.0029 (±0.0015) [*Sims et al.*, 1990]. The combined data for MORB and OIB showed the Sn/Sm ratio to be relatively constant at 0.36 (±0.08) [*Jochum et al.*, 1993]. Similarly, the Tl content can be estimated from a constant Rb/Tl ratio (230) in oceanic basalts [*McDonough and Sun*, 1995].

2.5. Major Element Composition of DM

[27] Thus far we have calculated a DM composition simply on the basis of the trace element and isotopic composition of the basalts. However, the determination of the major element composition of the DM reservoir cannot be based on the basalt composition alone. For example, the major element composition of a 10% melt from a 1% melt depleted source (compared to BSE) and a 10% melt of a 2% melt depleted source is very similar although the sources will have some differences in major element composition. Furthermore, the melting process is not understood well enough to relate basalt composition directly to source composition and another approach is needed.

[28] The radiogenic isotope systematics all indicate that the DM reservoir can be formed by extraction of 1−2% melt from BSE. Table 4 shows various estimates for the major element content of DM by extracting 1.0−1.5% melt from the BSE estimate from *McDonough and Sun* [1995]. The low degree melts (<2%) estimates are based on the experimental work of *Kinzler and Grove* [1992] at 1 GPa and the work of *Longhi* [2002] at 3 GPa. The pressure of melt extraction has a large effect on the major element composition of the melt, but the effect on major element content of the residue is minor. Most affected are SiO_2, Na_2O and FeO but even on those the possible range is limited (Table 4). Although direct mass balance with CC and the DM is not possible (see below), the steepness of the REE pattern in the CC indicates that some of the melting that formed CC took place in the presence of garnet [see also *Hofmann*, 1988]. Therefore we prefer a model whereby part of the depletion took place at high pressures. The rightmost column in Table 3 is the result of extraction of 1.5% melt from BSE of which half was extracted at 3 GPa and the other half at 1 GPa. This is our preferred model and

results in the preferred major element composition of the DM. We prefer 1.5% melt extraction because on the basis of the potassium content of the melts, no more than 1.5% of melt can be removed from BSE before potassium is quantitatively removed from the residue. Furthermore, on the basis of the isotopic compositions of MORB (and associated time integrated parent-daughter ratios) extraction of less than 1.5% will not produce large enough parent-daughter fractionations, unless the average age of the DM is increased to well over 3 Ga. Therefore our preferred model assumes 1.5% melt extraction, which agrees well with *Hofmann* [1988], and we consider this 1.5% to be relatively well constrained. However, regardless of the exact composition and amount of melt extracted (up to 2%), the range in composition of the melt residues is very limited with respect to major elements.

2.6. Trace Element Concentrations Derived From the Major Elements in Peridotites

[29] Several studies have shown that the chemical variations observed in anhydrous peridotite toward more depleted values than BSE are consistent with melting trends [*Hart and Zindler*, 1986; *McDonough and Sun*, 1995; *Zindler and Jagoutz*, 1988]. We used only anhydrous spinel lherzolites (data compilation courtesy of McDonough) as the chemical variations in this subset is more systematical and shows less scatter than the entire xenolith population which includes modally metasomatized peridotites. One might question the validity of peridotites from continental settings for the oceanic asthenosphere. In order to minimize differences between oceanic and continental settings we have excluded data from cratonic areas where most of the difference lies [*Boyd*, 1989] and concentrated on areas of relatively young CC (compared to the exposure age of the peridotite).

[30] Our estimates of the major element composition of DM can be used to determine additional trace element concentrations based on major-trace element correlations in peridotites. Although CaO is incompatible during melting, Table 3 shows that for small degrees of melting (at either high or low pressure), the differences in CaO content are insignificant compared to the possible range in Lu and Yb. We can now use the REE-major element variations in peridotites to obtain an absolute concentration for the Lu-content and thereby "fix" the concentrations of almost all of the trace elements (see Figure 1). Figure 6 shows the variations of Lu and Yb with CaO. With 3.5 wt% CaO for DM the Lu concentration is 63.4 ± 6 ppb; and this is the value where the trace element pattern in Figure 4 is anchored. Compared to BSE [*McDonough and Sun*, 1995] the degree of depletion of the HREE in the DM is limited and the HREE concentrations are only 8% lower than in BSE. This estimate is similar to what is obtained from removal of 1.5% of average CC from BSE.

[31] It has been shown that the MgO/Ni and Fe/Mn ratios are relatively constant in peridotites with values of 195 ± 20 and 60 ± 10, respectively [*McDonough and Sun*, 1995], and on the basis of the above determined MgO and FeO content of the DM we can calculate the Ni and Mn content of DM. Furthermore, the Cr-content in dry spinel peridotites is constant over a range of MgO and CaO contents and can be estimated to be 2500 ± 1000 ppm. With the CaO content of the DM, the correlations of CaO with Ga, Co, Sc, V, and Ag allow determination of their concentration: Ga = 3.1 ppm, Co = 106 ppm, Sc = 16.3 ppm, V = 79 ppm, Ag = 6 ± 3 ppb (see Figure 7 and Table 5). Of these elements, Ag is not constrained as well as the other elements because the CaO-Ag correlation is relatively poor and based on only 14 data points.

2.7. Platinum Group Element Concentrations

[32] Because platinum group elements (PGEs) partitioned into the metal phase during core formation the concentration of these elements in BSE is several orders of magnitude lower than in chondritic meteorites. However, their concentrations in BSE (or in peridotites) are higher than expected from metal-silicate partition experiments. Causes for the apparent enrichments are debated and could be either the addition of a late (after core formation) veneer of meteorites to the silicate Earth [*Morgan et al.*, 1981] or "bleeding" of the core into the mantle [*Brandon et al.*, 1998]. Furthermore, the CC has fractionated PGE ratios (high

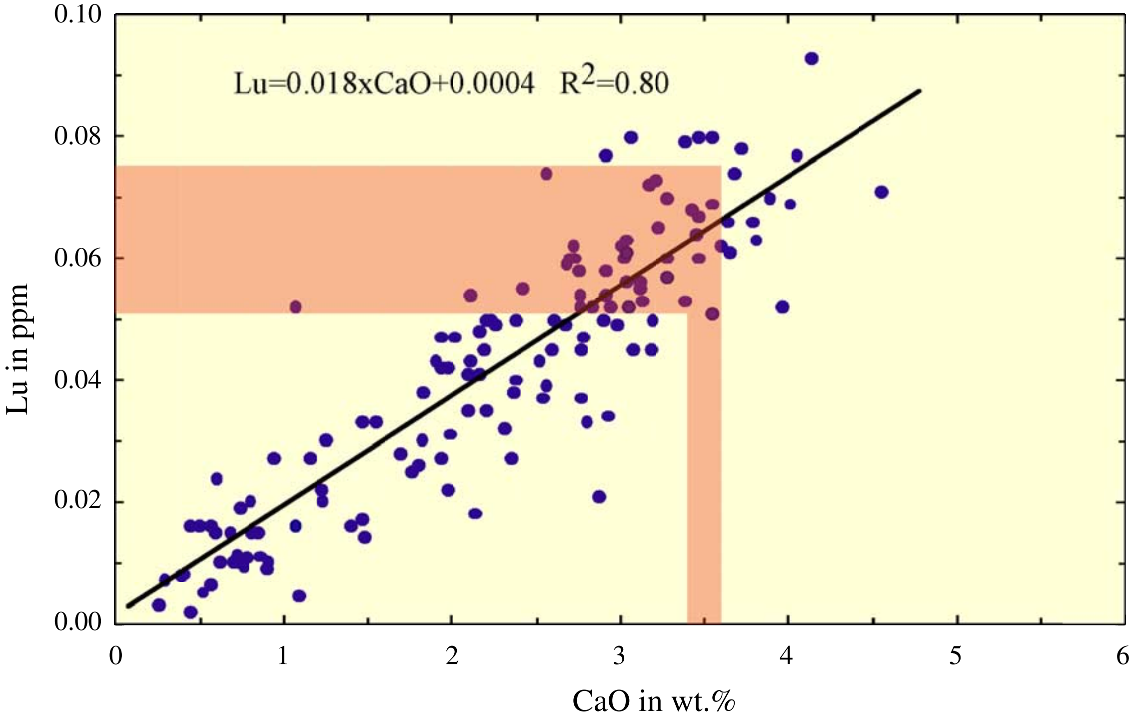

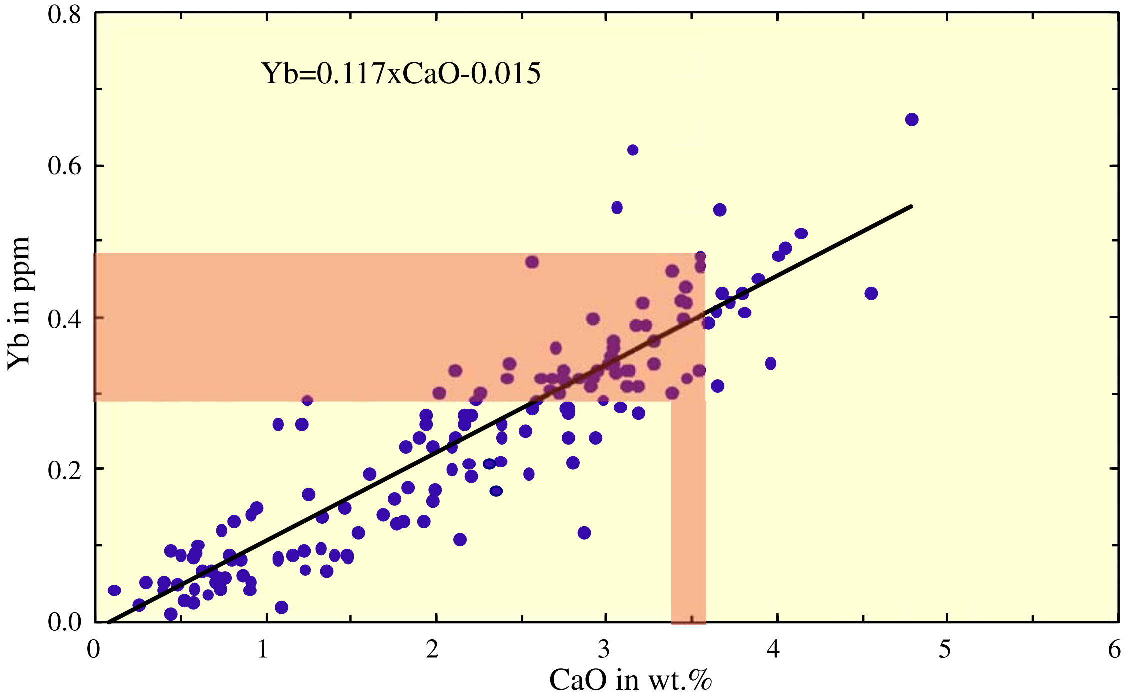

Figure 6. Yb and Lu variations with CaO in anhydrous spinel peridotites. Using 3.50 wt% CaO for the DM results in Yb and Lu concentrations only 8% lower than BSE.

Re/Os for example). Given these unknowns chondrites cannot be used to constrain either PGE concentrations or their ratios in DM. Most of the PGEs behave compatible during melting and the concentrations are higher in peridotites than in basalts. Therefore PGE concentrations in DM are better constrained using peridotites than basalts. There have been few studies on the concentrations

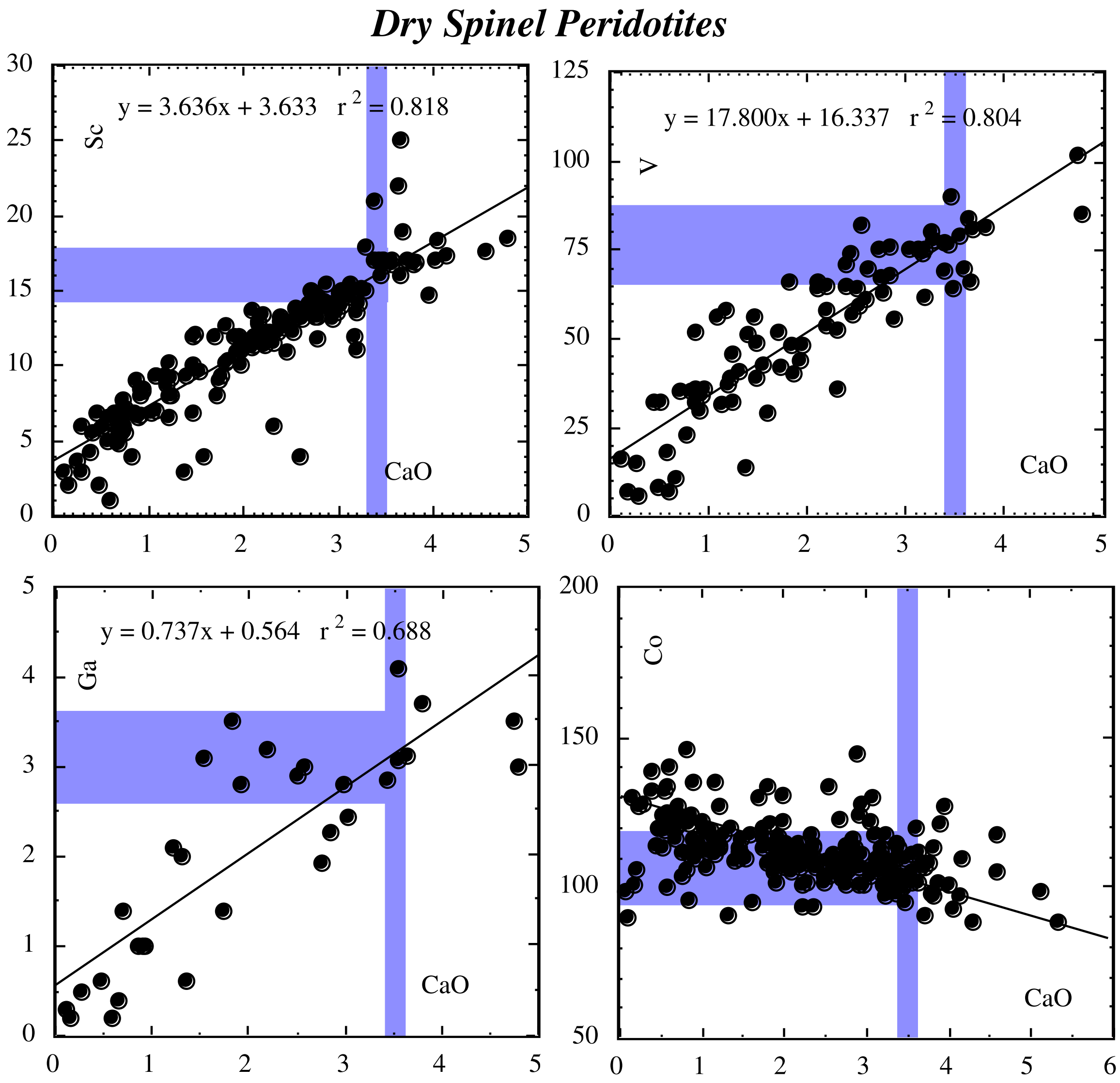

Figure 7. Trace element variations with CaO of anhydrous spinel peridotites.

of the PGEs in either basalts or peridotites that are useful to the characterization of the DM. These studies have shown relatively constant elemental ratios for most of the siderophile elements in abyssal peridotites [*Snow and Schmidt*, 1998], orogenic lherzolites [*Pattou et al.*, 1996] and ophiolites [*Snow et al.*, 2000], implying that the trace element ratios are constant over a large range of melting. Except for Re, which we will estimate using the Re-Os isotope systematics and Re/Yb in MORB, the PGE concentrations in DM were calculated as simple concentrations averages from the above cited lherzolite studies (Os = 2.99, Ir = 2.9, Ru = 5.7, Pt = 6.2, Rh = 1.02, Pd = 5.2, and Au = 0.99 ppb). Used in the table are the concentration ratios with respect to Ir so that the PGEs will vary consistently when the estimate for one of them is changed.

[33] The high Re/Os ratios and low Os concentrations in MORB [*Schiano et al.*, 1997] makes the Os-isotopic composition very sensitive to both alteration as well as eruption age. Uncertainty in eruption age of only several hundred thousand years has a large effect on the inferred Os-isotopic composition of the MORB source. Therefore the

Table 5. Elemental Ratios in the Continental Crust Compared With Ratios in PUM[a]

Ratio	PUM	CC	% Deviation
Ge/Si	5.2×10^{-6}	4.65×10^{-6}	11
Bi/Pb	0.0167	0.0164	2.1
Hg/Mn	9.6×10^{-6}	9.2×10^{-6}	3.5
Cu/Sc	1.85	1.23	33
Zn/Sc	3.4	3.29	3.3
Se/V	9.1×10^{-4}	9.4×10^{-4}	3.4
Be/Ta	1.84	2.7	32

[a] PUM from *McDonough and Sun* [1995] and continental crust from *Rudnick and Gao* [2003].

Os-isotopic composition of the MORB source and the associated Re/Os ratio have to be inferred from the least altered abyssal peridotites which still leaves a significant range: 0.1221–0.1272 [*Brandon et al.*, 2000; *Snow and Reisberg*, 1995]. In addition, the Os-isotopic composition of BSE has a large uncertainty, which affects the isotopic evolution of the DM. If BSE is similar to C-chondrites then BSE $^{187}Os/^{188}Os = 0.1268$ [*Luck and Allégre*, 1992]. If one assumes BSE is more similar to ordinary or enstatite chondrite, then $^{187}Os/^{188}Os = 0.129$ [*Meisel et al.*, 1996; *Shirey and Walker*, 1998]. Thus the constraints from the Os isotopic composition on the Re/Os of DM are not very strong. However, alternatively, the Re concentration is also constrained by constant Re/Yb ratios in basalts (327–475, ppt/ppm) [*Hauri and Hart*, 1997]. Using the Re/Yb ratio in basalts as a constraint and fixing the Os concentration at 2.99 ppt (see above) and the depletion age at 2.2 Ga and using the lowest $^{187}Os/^{188}Os$ value for BSE, the $^{187}Os/^{188}Os$ of the DM is between 0.120 and 0.123. The higher value for the $^{187}Os/^{188}Os$ BSE, with a 2.2 Ga depletion age, yields a the $^{187}Os/^{188}Os$ of the DM between 0.122 and 0.125. In either case the Re concentration has a similar range: 125–190 ppt. We have chosen the average of 157 ppt as the "recommended" value for the DM, leading to a present-day $^{187}Os/^{188}Os$ for DM of 0.1235.

2.8. Volatile Elements and Noble Gases

[34] Compared to major element or other trace element analyses there is only a relatively limited data set on the volatile elements (CO_2, H_2O, F, Cl, S) and relatively few estimates of the volatile content of the source composition have been made using the basalt glass data. The main issue to content with for the volatile elements is shallow level degassing. Two previous studies have estimated the H_2O content of DM on the basis of the similar compatibility of H_2O and the light REE: $H_2O/Ce = 155–213$ [*Michael*, 1995], $H_2O/La = 500$ [*Dixon et al.*, 1988]. A recent study on glass inclusions made great progress toward estimates of volatiles in DM through element ratios [*Saal et al.*, 2002]. Because these melt inclusions are preserved melts from a deeper part of the magmatic system than erupted glasses, the corrections and assumptions with regard to degassing are significantly less than in basalt glasses. The melt inclusions have been analyzed for some trace elements that make up the spider diagram as well as volatiles. These primitive melt inclusions show constant CO_2/Nb (230 ± 55), H_2O/Ce (168 ± 95), F/P (0.27 ± 0.11), S/Dy (225 ± 56) and Cl/K (0.010–0.007). Combined with the Nb, Ce, P, Dy and K estimates this now provides relatively accurate estimates for a number of the light elements.

[35] There is no rare gas data for melt inclusions, so for rare gases another approach is needed. There have been several estimates for the rare gas concentrations based on models of the solubility of the gases and their diffusion rates out of melts, but the estimates end up having relatively large uncertainties [*Cartigny et al.*, 2001; *Marty*, 1995; *Marty and Tolstikhin*, 1998; *Moreira and Allègre*, 1998; *Sarda and Graham*, 1990]. In general however these numbers are broadly consistent with what is observed in "popping rocks" [*Graham and Sarda*, 1991; *Javoy and Pineau*, 1991; *Sarda and Graham*, 1990]. The "popping rocks" are the least degassed ridge basalts and as such the least degassed samples from the DM. Consequently as a first approximation it can be assumed that the gases are present in concentration ratios that reflect their source composition. Furthermore, the trace elements as well as the radiogenic isotope ratios of these samples show in all respect MORB characteristics [*Bougault et al.*, 1988; *Dosso et al.*, 1991, 1993; *Sarda and Graham*, 1990]. Additionally the CO_2/Nb ratio is similar to *Saal et al.*'s [2002] determination on melt

inclusions. These lines of evidence indicate that volatile element ratios measured in these "popping rocks" are our best estimates for the DM. For the rare gas concentration estimates in Table 5 we have taken He/Ar, He/Ne, He/Kr and He/Xe from *Sarda and Graham* [1990], while we have taken C/He and C/N from *Javoy and Pineau* [1991]. The ratios reported in the publications are volume ratios, while the ratios reported in Table 5 are weight ratios.

2.9. Concentrations Derived From Continental Crust

[36] The above estimates, derived using either MORB or peridotite compositions, leave a number of elements of the periodic table undetermined. Of these remaining elements some constraints can be put on Cu, Zn, Ge, Hg, and Bi. These elements are not often measured in basalts or peridotites. Thus there is a lack of consistent data for these elements. By assuming that the CC is the reservoir that complements the DM we can use determinations of the CC for first order estimates of concentration in DM. We will see below that this is not strictly correct, but can serve as a rough approximation. Trace element ratios that are similar in the primitive mantle as well as in the CC can assumed to be also similar in DM. If the chondritic ratio in the CC involves an element whose concentration has previously been determined for the DM, we can make an estimate of the unknown element using the C1 value. One of the most obvious elements to use for this is Ge and Ge/Si. Ge and Si are thought to behave similar under a large range of conditions and their weight ratios in loess and waters is constant, identical and measured at 3.6×10^{-6} [*Mortlock and Froelich*, 1987] and this finding results Ge content of the DM of 0.76 ppm. Values for Ge/Si reported in the GERM reservoir base (http://earthref.sdsc.edu/) are derived from granitic rocks and these values are somewhat higher 4.5×10^{-6} to 4.8×10^{-6} resulting in estimates between 0.95 and 1.0 ppm of Ge in DM. The Ge content of BSE is estimated at 1.1 ppm [*McDonough and Sun*, 1995]. From Table 4 it can be seen that compared to the primitive mantle the depletion in SiO_2 in DM is relatively small. Consequently, we expect that the Ge depletion is of similar magnitude and we prefer the average of the two higher values (0.98 ppm) as a best estimate of the Ge content in DM. We have been able to find similar trace element ratios in CC and primitive mantle for trace element ratios that include some remaining elements. Table 5 shows ratios that are used to determine the concentration of the remaining elements. As our estimate for V, Sc and Mn content of DM is very similar to their content in PUM and the Se/V, Cu/Sc, Zn/Sc and Hg/Mn are very similar for PUM and CC [*Rudnick and Gao*, 2003] the estimated content for Cu, Zn, Se and Hg in DM is also close to the value in PUM. Bi/Pb and Be/Ta in the CC are similar to BSE values and as such we assume that Bi/Pb and Be/Ta in the DM is also similar to BSE [*McDonough and Sun*, 1995]. However, we have refrained from giving an error estimate on the estimate for these elements as those are clearly order of magnitude estimates. There is not enough data for I, Te, and Br to allow an accurate estimate for these elements.

3. Discussion

[37] Table 6 provides our estimate for the concentrations in the DM of most elements of the periodic table, and Figure 1 shows schematically how these estimates are obtained and what the dependencies are. Table 6 also provides an estimate of the uncertainty in the concentration of each elements in the DM. The uncertainty is calculated as one standard deviation of the elemental ratio used to make the estimate. For example, the Sm concentration is derived from Sm/Hf in primitive MORB which has one standard deviation of 10%. To obtain the complete range of Sm concentrations possible one has to add the uncertainty in the estimate of the Hf concentration (through the Lu/Hf ratio) and the uncertainty in Lu concentration. The further down the elements in Figure 1, the more estimates need to be combined to obtain a concentration estimate and thus more uncertainties are accumulated. The accompanying spreadsheet with averages of concentrations and concentration ratios also provides standard deviations for the D-MORB compilation used to construct the spider diagram. It is clear that

Table 6. Estimate of the Composition of the Depleted Mantle

Element	Model	Unit	Constraint	Uncertainty in %	Element	Model	Unit	Constraint	Uncertainty in %
H_2O	116	ppm	H_2O/Ce	50	Ru	5.7	ppb	Ir/Ru	16
He	157	ppt	C/He	46	Rh	1.0	ppb	Ir/Rh	15
Li	0.70	ppm	Yb/Li	8	Pd	5.2	ppb	Ir/Pd	24
Be	25	ppb	Be/Ta	100	Ag	6	ppb	Ag-CaO	50
B	0.060	ppm	B/K	91	Cd	0.014	ppm	Cd/Dy	30
CO_2	50.3	ppm	CO_2/Nb	24	In	12.2	ppb	In/Y	25
N_2	40	ppb	C/N	30	Sn	0.10	ppm	Sn/Sm	22
F	11.0	ppm	F/P	41	Sb	2.6	ppb	Sb/Pr	42
Ne	30.7	ppq	He/Ne	40	Te	15.1	ppb	Te/Ni	80
Na_2O	0.29	wt%	MMM	10	Xe	0.79	ppq	He/Xe	40
MgO	38.22	wt%	MMM	1	Cs	1.32	ppb	Cs/Rb	42
Al_2O_3	4.28	wt%	MMM	2	Ba	1.20	ppm	Rb/Ba	49
SiO_2	44.9	wt%	MMM	1	La	0.234	ppm	La/Ce	14
P	40.7	ppm	Ce/P	25	Ce	0.772	ppm	Ce/Nd	15
S	119	ppm	S/Dy	25	Pr	0.131	ppm	Nd/Pr	10
Cl	0.51	ppm	Cl/K	18	Nd	0.713	ppm	Sm/Nd	7
Ar	1.21	ppb	He/Ar	38	Sm	0.270	ppm	Sm/Hf	10
K	60	ppm	K/U	28	Eu	0.107	ppm	Eu/Lu-Sm	10
CaO	3.5	wt%	MMM	1	Gd	0.395	ppm	Gd/Lu-Sm	10
Sc	16.3	ppm	Sc-CaO	13	Tb	0.075	ppm	Tb/Lu-Sm	10
Ti	798	ppm	Ti/Gd	12	Dy	0.531	ppm	Dy/Lu-Sm	10
V	79	ppm	CaO-V	7	Ho	0.122	ppm	Ho/Lu-Sm	10
Cr	2500	ppm	CaO-Cr	40	Er	0.371	ppm	Er/Lu-Sm	10
Mn	1045	ppm	Fe/Mn	17	Tm	0.060	ppm	Tm/Lu-Sm	10
FeO	8.07	wt%	MMM	2	Yb	0.401	ppm	Yb/Lu-Sm	7
Co	106	ppm	Co-CaO	14	Lu	0.063	ppm	Lu-CaO	9
Ni	1960	ppm	MgO/Ni	10	Hf	0.199	ppm	Lu/Hf	8
Cu	30	ppm	Cu/Sc		Ta	13.8	ppb	Nb/Ta	33
Zn	56	ppm	Zn/Sc		W	3.5	ppb	W/Ba	52
Ga	3.2	ppm	CaO	16	Re	0.157	ppb	Re/Os	25
Ge	1.0	ppm	Ge/Si	200	Os	2.99	ppb	Os/Ir	15
As	7.4	ppb	As/Ce	28	Ir	2.9	ppb	Per	20
Se	72	ppb	Se/V		Pt	6.2	ppb	Ir/Pt	27
Kr	2	ppq	He/Kr	40	Au	1.0	ppb	Ir/Au	48
Rb	0.088	ppm	Rb/Sr	25	Hg	10	ppb	Hg/Mn	
Sr	9.80	ppm	Sr/Nd	19	Tl	0.38	ppb	Rb/Tl	
Y	4.07	ppm	Y/Yb	12	Pb	23.2	ppb	Th/Pb	30
Zr	7.94	ppm	Zr/Hf	22	Bi	0.39	ppb	Bi/Pb	
Nb	210	ppb	U/Nb	35	Th	13.7	ppb	Ba/Th	30
Mo	25	ppb	Mo/Ce	28	U	4.7	ppb	Th/U	30

the range in most elements is quite large. Even for a "well behaved" trace element ratio like Sm/Hf the two standard variation is still 20%, which results in a relatively large uncertainty.

[38] Absolute uncertainties on trace elements other than those used in the "standard" spider diagram are in general larger and a factor of two uncertainty can generally be assumed. The reader is advised to consult the original papers for a detailed description of the estimates. Uncertainties in the major element estimate are relatively small (see Table 3). Assuming that the depletion event is 1–2% melt extraction the major element composition is known to within several percent, except for sodium and potassium, which have estimated absolute uncertainties of about 20% and 50%, respectively.

[39] As our estimates are partly based on our preconceived notions, we have also added a spreadsheet ("DM GERM.xls") in which the composition and relationships between elemental concentrations is condensed. This spreadsheet is basically an implementation of Figure 1 and is a

tool to determine the consequence of a change of one concentration or concentration ratio on other elements.

[40] Previously it has been argued that major elements and moderately incompatible trace elements indicate that CC and DM are complementary reservoirs related to each other through partial melting [*Hofmann*, 1988; *Hofmann et al.*, 1986a]. However, with our current estimate of MORB and DM it becomes difficult to support this notion. Figure 8 shows the trace element patterns for the DM and compares it with the calculated trace element patterns for small degree melts from a chondritic source. The partition coefficients, modes, and melt reactions are given in Table 7 and are based on experimental data of *Salters et al.* [2002] and *Salters and Longhi* [1999] as well as the compilation of *Halliday et al.* [1995]. It can be seen that the trace element concentration of the incompatible elements in the melts is higher (U through Gd) than in the average CC. Conversely, a reservoir formed by extraction of 1% CC has concentrations for the elements U through Gd that are too low for it to be a possible source for MORB. The steepness of the DM pattern is dictated by the average age of the source. Using the oldest average age results in the least steep spider pattern. However, even increasing the age of the source to 4.55 Ga will not result in overlap between calculated residues of CC extraction and calculated MORB sources.

[41] Another approach to determine whether DM and CC are complementary is simple mass balance of bulk silicate Earth (BSE) and CC whereby the DM is assumed to be the residue of CC extraction [*Hofmann*, 1988]. This requires knowledge of the size of the reservoirs, which for the DM reservoir has a large uncertainty [*Zindler and Hart*, 1986]. First one can calculate how much CC needs to be removed from BSE to fractionate Sm/Nd and Lu/Hf enough to create the depleted isotope signatures in MORB. This simple mass balance requires that approximately 2% of CC needs to be removed from a chondritic reservoir approximately 3.0 Ga ago to produce the isotopic composition of D-MORB or All-MORB. This fraction increases for younger average ages of the depletion event. Removal of a smaller fraction of continental crust requires an even older average age for the MORB source as the Sm/Nd and Lu/Hf ratios are less fractionated. A problem created by this approach is that removal of more than 1–1.5% of CC from a chondritic BSE results in deficits in the residual mantle for all Large Ion Lithophile Elements (LIL elements, K to Cs). Therefore the simple mass balance with CC does not seem to be able to satisfy all the isotopic and trace element constraints simultaneously.

[42] Figure 8 also shows melts and residual compositions of small-degree melts from a reservoir with BSE trace element contents. The patterns of melts derived from the garnet stability field (3 GPa) fit the CC pattern slightly better than the patterns of melts derived from the spinel stability field (2 GPa). The difference between using batch and fractional melting is largest for the highly incompatible elements, and in order to retain relatively high concentrations for the highly incompatible elements in the residue, batch melting with some melt left in the residue is required. This observation is confirmed by the Th/U ratio of the residue. In order for Th/U in the residue (MORB source) to be approximately 2.5–3.0 batch melting with some melt being retained in the residue is required, whether the melting takes place in the garnet or in the spinel stability field. These model calculations suggest that the CC can be approximated by a small degree melt although the "fit" is not perfect. This is perhaps not surprising as part of the CC formation occurs in island arc settings where material different from BSE melts to form crust and where the degree of melting is thought to be greater than 2%.

[43] It has also been argued that the DM is not the complement of CC extraction, or a small degree of melt extraction, but is BSE-type mantle with the addition of depleted material that is residual after oceanic crust formation [*Campbell*, 2002]. However, this model fails to explain the low Th/U of

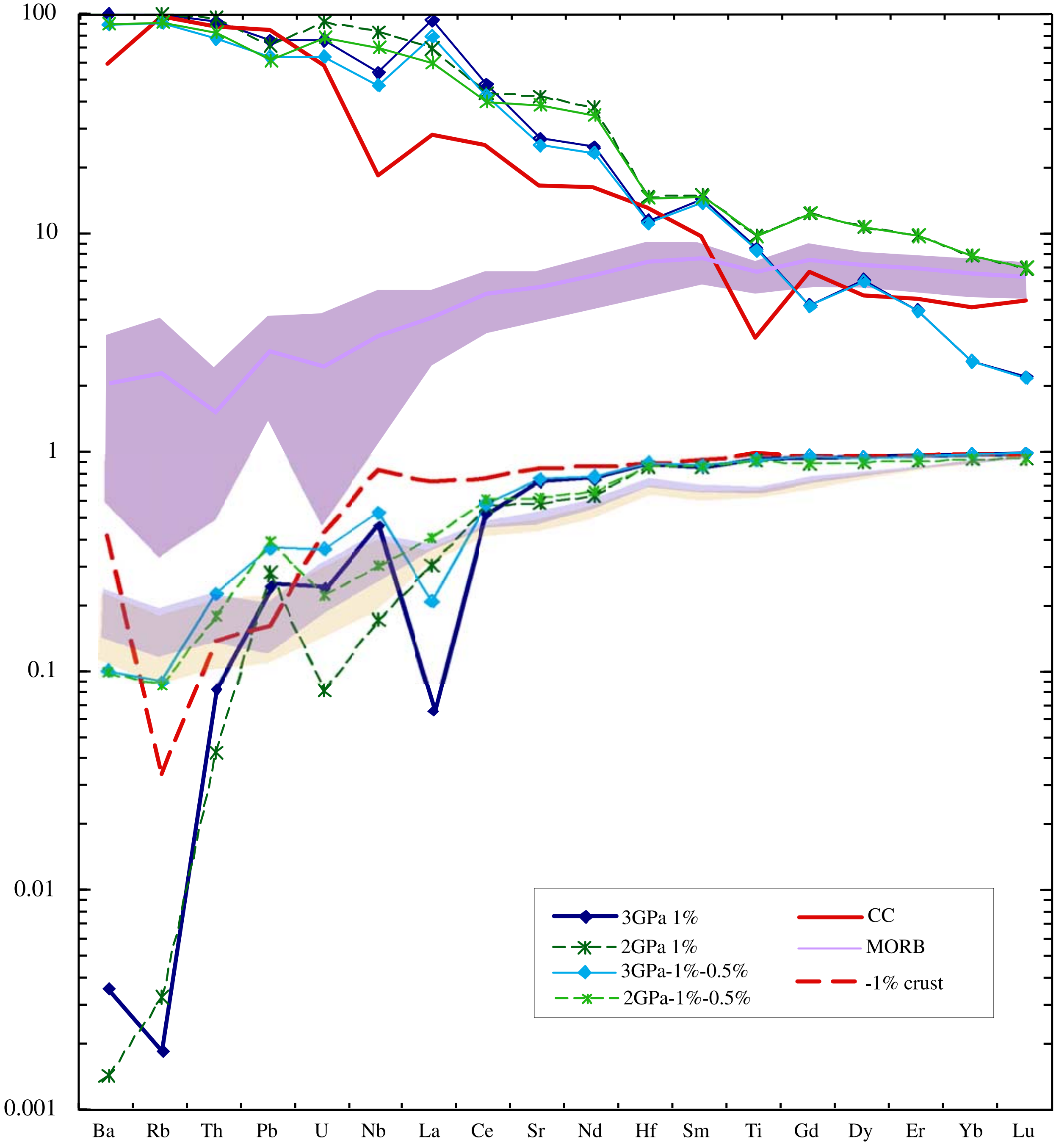

Figure 8. Comparison of the different types of models to estimate the composition of the DM by extraction of crust or small degree melt. Dark blue and dark green patterns are the results for pure fractional melting (melts and corresponding residues), while light blue and light green represent 1% fractional melts, but 0.5% melt is kept in the residue. Blue and orange shaded areas are the range of calculated DM compositions from this paper. The blue area is for average and orange is for extreme isotopic compositions. The purple pattern is D-MORB; the purple area is D-MORB pattern with its observed variation (2 standard deviation; see spreadsheet D-MORB-comp.xls). Abundances are normalized to BSE [*McDonough and Sun*, 1995].

Table 7. Partition Coefficients, Mineral Modes, and Melt Reactions

	3 GPa				2 GPa[a]		
	Olivine	opx	cpx	Garnet	Olivine	opx	cpx
Cs	0	0	0	0	0	0	0
Rb	0.0003	0.0002	0.0004	0.0002	0.0003	0.0002	0.0004
Ba	0.000005	0.000006	0.0004	0.00007	0.000005	0.000006	0.000400
Th	0.00005	0.002	0.00566	0.009	0.00005	0.002	0.00590
Pb	0.003	0.009	0.009	0.005	0.003	0.009	0.012
U	0.00038	0.002	0.0113	0.028	0.00038	0.002	0.0094
K	0.00002	0.0001	0.001	0.013	0.00002	0.0001	0.001
Ta	0.0005	0.004	0.01	0.015	0.0005	0.004	0.015
Nb	0.0005	0.004	0.01	0.015	0.0005	0.004	0.015
La	0.0005	0.004	0.015	0.0007	0.0005	0.0031	0.03
Ce	0.0005	0.004	0.038	0.017	0.0005	0.004	0.08
Sr	0.00004	0.0007	0.091	0.0007	0.00004	0.0007	0.091
Nd	0.00042	0.012	0.0884	0.064	0.00042	0.012	0.088
Hf	0.0011	0.024	0.1400	0.4	0.0022	0.03	0.2835
Sm	0.0011	0.02	0.1509	0.23	0.0011	0.02	0.299
Ti	0.015	0.086	0.14	0.6	0.015	0.086	0.350
Gd	0.0011	0.065	0.16	1.2	0.0011	0.0065	0.350
Dy	0.0027	0.065	0.17	2	0.0027	0.011	0.400
Er	0.013	0.065	0.18	3	0.013	0.045	0.420
Yb	0.02	0.08	0.25	5.5	0.020	0.08	0.450
Lu	0.02	0.12	0.276	7	0.020	0.12	0.511
Mineral modes	0.53	0.08	0.34	0.05	0.53	0.29	0.18
Melt reaction	−0.05	0.49	−1.31	−0.13	−0.375	0.5	−1.125

[a] Spinel is considered to be inert and has very low partition coefficients for these incompatible elements and is ignored in the calculations.

the DM unless large amounts of material residual after oceanic crust formation is part of the MORB source. The Th/U ratio provides relatively strong constraints on the origin of the DM [see also *Turcotte et al.*, 2001]. Material residual after MORB generation has 50–100 times lower U-Th concentration than BSE (with Th/U = 4). Although the Th/U in this residual material is also low (Th/U = 0.5–0.2) still large amounts of this material is needed (80–90%) to obtain the Th/U of 2.9 calculated for DM.

[44] Figure 3 shows that the LIL content in primitive MORB is 13–15 times higher than the estimates for the source. If these elements behave perfectly incompatible during melting, then on average MORB are generated by less than 10% melting. With best estimates for the partition coefficients (Table 7) and best estimates for the style of melting [*Salters et al.*, 2002] the preferred DM trace element pattern from Figure 3 can yield MORB by about 8–10% of melting which is similar to previous estimates [*Johnson et al.*, 1990; *Klein and Langmuir*, 1987]. The patterns for source compositions required for the production of MORB using different degrees of melting are shown in Figure 9. The source compositions that yield MORB through 8–15% of melting fits the calculated DM composition based on isotope and trace element patterns the best.

[45] As the water content of the mantle influences the viscosity as well as the conductivity it seems justified to critically examine the estimate of the water content of the depleted mantle. Our preferred value of 116 ppm H_2O (range of 50–180 ppm, using the full range of observed H_2O/Ce ratios) is similar to earlier estimates [*Dixon et al.*, 2002; *Michael*, 1995]. If the extreme isotopic compositions are used then the average age of the depletion and the calculated water content will decrease by about 10% while still satisfying all other constrains. Similarly, lowering the $^{87}Sr/^{86}Sr$ of BSE to 0.704 again will result in a 10% lowering of the H_2O estimate. It thus seems that the estimate for

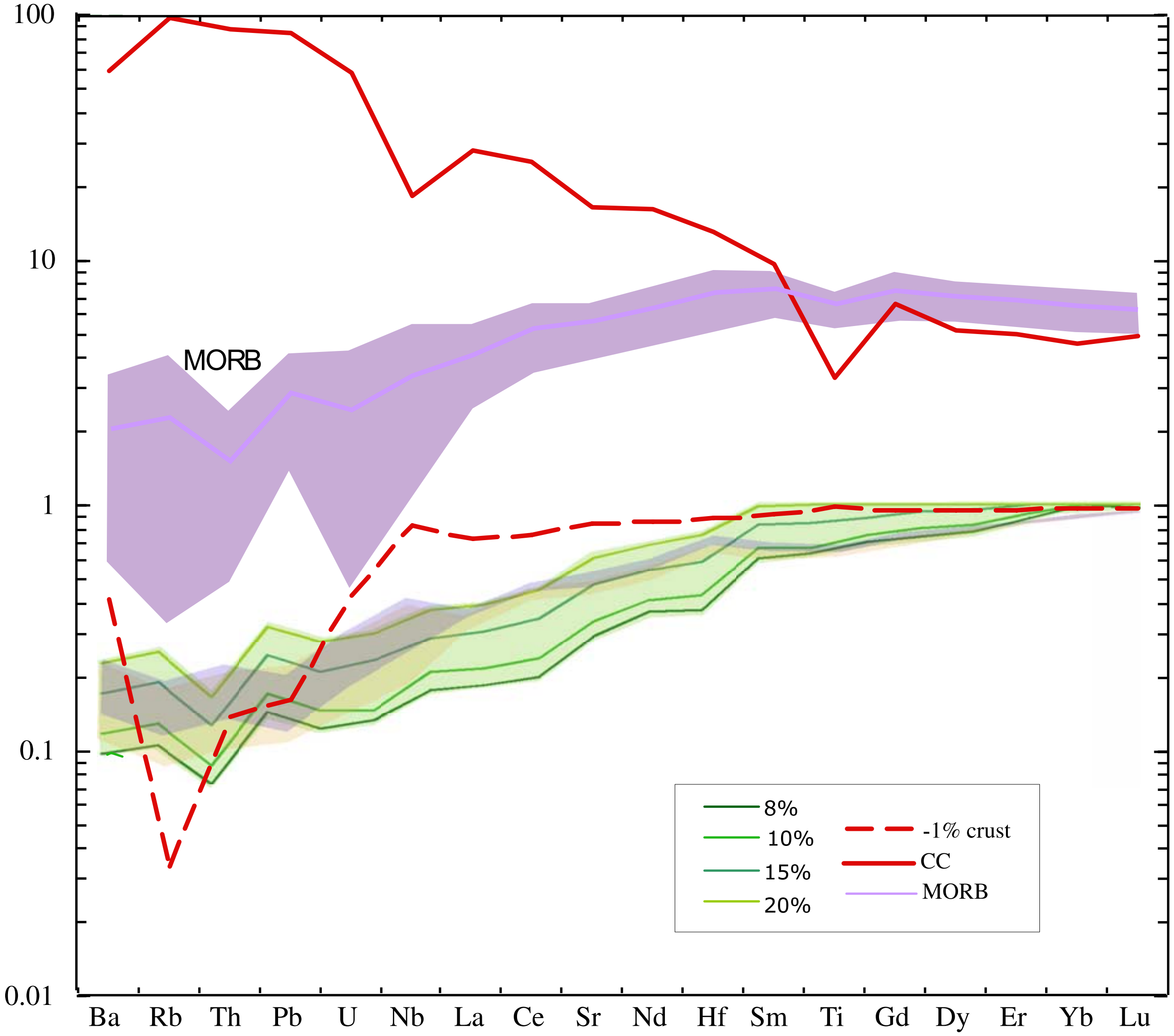

Figure 9. Comparison of the DM based on the trace element ratios in basalt and those based on melting models (green). Shown are calculated DM compositions that will yield D-MORB (purple pattern) for 8 to 20% melting. Shaded blue and orange fields are DM estimates from this paper as in Figure 8. The purple pattern is D-MORB; the purple area is D-MORB pattern with its observed variation (2 standard deviation; see spreadsheet D-MORB-comp.xls). Abundances are normalized to BSE [*McDonough and Sun*, 1995].

the water content provided in Table 6 is on the high side.

Appendix A: Description of Dynamic Content

[46] The manuscript has two Microsoft Excel files attached: Tables A1 and A2. Table A1 contains the data used to obtain the average MORB composition. This file contains three worksheets. "References" contains the references for the data given by the PetDB database. "Samples" contains the chemical data and the keyed reference for the samples used in the estimate. Rows 141 through 148 of this worksheet contain the ridge segment average of the southern Mid-Atlantic Ridge, based on the data of Le Roux et al., reference 1107 and 1110 of the PetDB database. Worksheet "EWI9309" contains the data on which the segment averages from rows 141 through 148 of the

"Samples" worksheet are based. The "Samples" worksheet also provides the average and the median as well as the standard deviation for the MORB estimate for both elemental abundances as well as trace element ratios that are used to calculate the DM composition.

[47] The second Microsoft Excel file, Table A2, contains three separate worksheets. The first worksheet, "Periodic table D-MORB," is the worksheet implementation of Figure 1 using the D-MORB estimate from the Table A1 file. The calculated composition is displayed in the orange box in the columns labeled "model," and these values are fixed. Changes in the constraining ratios (columns "F" and "L") result in changes in the values in the "Active" columns. The constraints derived from the isotopic compositions are described in the blue box and are linked to the appropriate ratios in the orange box. Changes in the isotope ratios (row "MORB now" or changes in the average depletion age ("X in years") result in changes in the constraining ratios and in the linked "active" cells. Some changes in the constraints will result in changes in Ce/Pb, La/Nb, and Re/Yb. These ratios are displayed in the red box and for a viable model the "active" values should stay within the minimum and maximum.

[48] The worksheets labeled "All MORB La < 5" and "All-MORB" provide estimates based on the alternative compilations.

Acknowledgments

[49] Hubert Staudigel is thanked for initially proposing this project. Pierre Cartigny is thanked for advising on the volatile content. Thanks to David Graham, Bill McDonough and Bill White as their reviews resulted in significant improvements of the manuscript. This publication is supported by NSF grant EAR 0124965 to VS.

References

Albarède, F., and M. Brouxel (1987), The Sm/Nd secular evolution of the continental crust and depleted mantle, *Earth Planet. Sci. Lett.*, *82*, 25–35.

Allègre, C. J., J.-L. Birck, S. Fourcade, and M. P. Semet (1975), Rubidium-87/strontium-87 age of Juvinas basaltic achondrite and early igneous activity in the solar system, *Science*, *187*, 436–438.

Allègre, C. J., S. R. Hart, and J. F. Minster (1983a), Chemical structure and evolution of the mantle and the continents determined by inversion of Nd and Sr isotopic data, I. Theoretical models, *Earth Planet. Sci. Lett.*, *66*, 177–190.

Allègre, C. J., S. R. Hart, and J. F. Minster (1983b), Chemical structure and evolution of the mantle and the continents determined by inversion of Nd and Sr isotopic data, II. Numerical experiments and discussion, *Earth Planet. Sci. Lett.*, *66*, 191–213.

Batiza, R. (1984), Inverse relationship between Sr isotope diversity and rate of oceanic volcanism has implications for mantle heterogeneity, *Nature*, *309*, 440–441.

Bougault, H., L. Dmitriev, J. G. Schilling, A. Sobolev, J. L. Joron, and H. D. Needham (1988), Mantle heterogeneity from trace elements: MAR triple junction near 14°N, *Earth Planet. Sci. Lett.*, *88*, 27–36.

Bourdon, B., A. Zindler, C. H. Langmuir, and J. F. Bender (1993), U-Th systematics of MORB near the Tamayo transform at 22°30N, EPR: Implications for melting processes, *Eos Trans. AGU*, *74*, 632.

Bourdon, B., C. H. Langmuir, and A. Zindler (1996), Ridge-hotspot interaction along the Mid-Atlantic Ridge between 37°30 and 40°30N: The U-Th disequilibrium evidence, *Earth Planet. Sci. Lett.*, *142*, 175–190.

Boyd, F. R. (1989), Compositional distinction between oceanic and cratonic lithosphere, *Earth Planet. Sci. Lett.*, *96*, 15–26.

Brandon, A. D., R. J. Walker, J. W. Morgan, M. D. Norman, and H. M. Prichard (1998), Coupled ^{186}Os and ^{187}Os evidence for core-mantle interaction, *Science*, *280*, 1570–1573.

Brandon, A. D., J. E. Snow, R. J. Walker, J. W. Morgan, and T. D. Mock (2000), ^{190}Pt-^{186}Os and ^{187}Re-^{187}Os systematics in abyssal peridotites, *Earth Planet. Sci. Lett.*, *177*, 319–335.

Campbell, D. H. (2002), Implications of Nb/U, Th/U and Sm/Nd in plume magmas for the relationship between continental and oceanic crust formation and the development of the depleted mantle, *Geochim. Cosmochim. Acta*, *66*(9), 1651–1661.

Cartigny, P., N. Jendrzejewski, F. Pineau, F. Petit, and M. Javoy (2001), Volatile (C, N, Ar) variability in MORB and the respective roles of mantle source heterogeneity and degassing: The case of the Southwest Indian Ridge, *Earth Planet. Sci. Lett.*, *194*, 241–257.

Chase, C. G., and P. J. Patchett (1988), Stored mafic/ultramafic crust and early Archean mantle depletion, *Earth Planet. Sci. Lett.*, *91*, 66–72.

Christie, D. M., B. P. West, D. G. Pyle, and B. B. Hanan (1998), Chaotic topography, mantle flow and mantle migration in the Australian-Antarctic discordance, *Nature*, *394*, 637–644.

Condie, K. C. (2000), Episodic continental growth models: Afterthoughts and extensions, *Tectonophysics*, *322*(1–2), 153–162.

Condomines, M., P. Morand, and C. J. Allègre (1981), ^{230}Th-^{238}U radioactive disequilibria in tholeiites from the FAMOUS zone (Mid-Atlantic Ridge, 36°50′N): Th and Sr isotopic geochemistry, *Earth Planet. Sci. Lett.*, *55*, 247–256.

DePaolo, D. J. (1980), Crustal growth and mantle evolution: Inferences from models of element transport and Nd and Sr isotopes, *Geochim. Cosmochim. Acta*, *44*, 1185–1196.

Dixon, J. E., E. Stolper, and J. R. Delaney (1988), Infrared spectroscopic measurements of CO_2 and H_2O in Juan de Fuca Ridge basaltic glasses, *Earth Planet. Sci. Lett.*, *90*, 87–104.

Dixon, J. E., L. Leist, C. H. Langmuir, and J.-G. Schilling (2002), Recycled dehydrated lithosphere observed in plume-influenced mid-ocean-ridge basalts, *Nature*, *420*, 385–389.

Dosso, L., B. B. Hanan, H. Bougault, J.-G. Schilling, and J.-L. Joron (1991), Sr-Nd-Pb geochemical morphology between 10° and 17°N on the Mid-Atlantic Ridge: A new MORB isotope signature, *Earth Planet. Sci. Lett.*, *106*, 29–43.

Dosso, L., H. Bougault, and J.-L. Joron (1993), Geochemical morphology of the north Mid-Atlantic Ridge, 10°–24°N: Trace element-isotope complementary, *Earth Planet. Sci. Lett.*, *120*, 443–462.

Dupré, B., and C. J. Allègre (1983), Pb-Sr isotope variation in Indian Ocean and mixing phenomena, *Nature*, *303*, 142–146.

Elliott, T., A. Zindler, and B. Bourdon (1999), Exploring the kappa conundrum: The role of recycling in the lead isotope evolution of the mantle, *Earth Planet. Sci. Lett.*, *169*, 129–145.

Galer, S. J. G., and R. K. O'Nions (1985), Residence time of thorium, uranium and lead in the mantle with implications for mantle convection, *Nature*, *316*, 778–782.

Galer, S. J. G., S. L. Goldstein, and R. K. O'Nions (1989), Limits on chemical and convective isolation in the Earth's interior, *Chem. Geol.*, *75*, 257–290.

Goldstein, S. J., M. T. Murrell, and D. R. Janecky (1989), Th and U isotopic systematics of basalts from the Juan de Fuca and Gorda Ridges by mass spectrometry, *Earth Planet. Sci. Lett.*, *96*, 134–146.

Goldstein, S. J., M. T. Murrell, D. R. Janecky, J. R. Delaney, and D. A. Clague (1991), Geochronology and petrogenesis of MORB form the Juan de Fuca and Gorda ridges by ^{238}U-^{230}Th disequilibrium, *Earth Planet. Sci. Lett.*, *107*, 25–41.

Goldstein, S. J., M. T. Murrell, and R. W. Williams (1993), ^{231}Pa and ^{230}Th chronology of mid-ocean ridge basalts, *Earth Planet. Sci. Lett.*, *115*, 151–159.

Goldstein, S. J., M. R. Perfit, R. Batiza, D. J. Fornari, and M. T. Murrell (1994), Off-axis volcanism at the East Pacific Rise detected by uranium-series dating of basalts, *Nature*, *367*, 157–159.

Graham, D., and P. Sarda (1991), Reply to comment by T. M. Gerlach on "Mid-ocean ridge popping rocks: Implications for degassing at ridge crests,", *Earth Planet. Sci. Lett.*, *105*, 568–573.

Graham, D. W., A. Zindler, M. D. Kurz, W. J. Jenkins, R. Batiza, and H. Staudigel (1988), He, Pb, Sr and Nd isotope constraints on magma genesis and mantle heterogeneity beneath young Pacific seamounts, *Contrib. Mineral. Petrol.*, *99*, 446–463.

Halliday, A. N., D.-C. Lee, S. Tommasini, G. R. Davies, C. R. Paslick, J. G. Fitton, and D. E. James (1995), Incompatible trace elements in OIB and MORB and source enrichment in the sub-oceanic mantle, *Earth Planet. Sci. Lett.*, *133*, 379–395.

Hanan, B. B., J. Blichert-Toft, D. G. Pyle, D. Christie, and F. Albarède (2000), Ultra-depleted hafnium isotopes from Australian-Antarctic discordance MORB, *J. Conf. Abstr.*, *5*(2), 478–479.

Hart, S. R. (1984), The DUPAL anomaly: A large scale isotopic mantle anomaly in the Southern Hemisphere, *Nature*, *309*, 753–757.

Hart, S. R., and A. Zindler (1986), In search for bulk-earth composition, *Chem. Geol.*, *57*, 247–267.

Hauri, E. H., and S. R. Hart (1997), Rhenium abundances and systematics in oceanic basalts, *Chem. Geol.*, *139*(1–4), 185–205.

Hofmann, A. W. (1986), Nb in Hawaiian magmas: Constraints on source composition and evolution, *Chem. Geol.*, *57*, 17–30.

Hofmann, A. W. (1988), Chemical differentiation of the Earth: The relationship between mantle, continental crust, and oceanic crust, *Earth Planet. Sci. Lett.*, *90*, 297–314.

Hofmann, A. W. (1997), Mantle geochemistry: The message from oceanic volcanism, *Nature*, *385*, 219–229.

Hofmann, A. W., and W. M. White (1982), Mantle plumes from ancient oceanic crust, *Earth Planet. Sci. Lett.*, *57*, 421–436.

Hofmann, A. W., and W. M. White (1983), Ba, Rb and Cs in the Earth's mantle, *Z. Naturforsch.*, *38a*, 256–266.

Hofmann, A. W., K. P. Jochum, H. M. Seufert, and W. M. White (1986a), Nb and Pb in oceanic basalts: New constraints on mantle evolution, *Earth Planet. Sci. Lett.*, *79*, 33–45.

Hofmann, A. W., K. P. Jochum, M. Seufert, and W. M. White (1986b), Nb and Pb in oceanic basalts: New constraints on mantle evolution, *Earth Planet. Sci. Lett.*, *79*, 33–45.

Jagoutz, E., H. Palme, H. Baddenhausen, K. Blum, M. Cendales, G. Dreibus, B. Spettel, V. Lorenz, and H. Wanke (1979), The abundances of major, minor and trace elements in the Earth's mantle as derived from primitive ultramafic nodules, *Proc. Lunar. Planet. Sci. Conf. 10th*, 2031–2050.

Javoy, M., and F. Pineau (1991), The volatiles record of a "popping" rock from the Mid-Atlantic Ridge at 14°N: Chemical and isotopic composition of gas trapped in vesicles, *Earth Planet. Sci. Lett.*, *107*, 598–611.

Jochum, K. P., and A. W. Hofmann (1997), Constraints on Earth evolution from antimony in mantle-derived rocks, *Chem. Geol.*, *139*(1–4), 39–49.

Jochum, K. P., A. W. Hofmann, E. Ito, H. M. Seufert, and W. M. White (1983), K, U and Th in mid-ocean ridge basalt glasses: The terrestrial K/U and K/Rb ratios and the heat production in the depleted mantle, *Nature*, *306*, 431–436.

Jochum, K. P., H. M. Seufert, B. Spettel, and H. Palme (1986), The solar-system abundances of Nb, Ta, and Y, and the relative abundances of refractory lithophile elements in differentiated planetary bodies, *Geochim. Cosmochim. Acta*, *50*, 1173–1183.

Jochum, K. P., N. T. Arndt, and A. W. Hofmann (1991), Nb-Th-La in komatiites and basalts: Constraints on komatiite petrogenesis and mantle evolution, *Earth Planet. Sci. Lett.*, *107*, 272–289.

Jochum, K. P., A. W. Hofmann, and H. M. Seufert (1993), Tin in mantle-derived rocks: Constraints on Earth evolution, *Geochim. Cosmochim. Acta*, *57*, 3585–3595.

Johnson, K. T. M., and H. J. B. Dick (1992), Open system melting and temporal and spatial variation of peridotite and basalt at the Atlantis II fracture zone, *J. Geophys. Res.*, *97*, 9219–9241.

Johnson, K. T. M., H. J. B. Dick, and N. Shimizu (1990), Melting in the oceanic upper mantle: An ion microprobe study of diopsides in abyssal peridotites, *J. Geophys. Res.*, *95*, 2661–2678.

Kinzler, R. J., and T. L. Grove (1992), Primary magmas of mid-ocean ridge basalts: 2. Applications, *J. Geophys. Res.*, *97*, 6907–6926.

Klein, E. M., and C. H. Langmuir (1987), Global correlations of ocean ridge basalt chemistry with axial depth and crustal thickness, *J. Geophys. Res.*, *92*, 8089–8115.

Klein, E. M., C. H. Langmuir, A. Zindler, H. Staudigel, and B. Hamelin (1988), Isotopic evidence of a mantle convection boundary at the Australian-Antarctic Discordance, *Nature*, *333*, 623–629.

Kleine, T., C. Münker, K. Mezger, and H. Palme (2002), Rapid accretion and early core formation on asteroids and the terrestrial: Planets from Hf-W chronometry, *Nature*, *418*, 952–955.

Longhi, J. (2002), Some phase equilibrium systematics of lherzolite melting: I, *Geochem. Geophys. Geosyst.*, *3*(3), 1020, doi:10.1029/2001GC000204.

Luck, J. M., and C. J. Allégre (1992), Osmium isotopes in ophiolites, *Earth Planet. Sci. Lett.*, *107*, 406–415.

Lundstrom, C. C., Q. Williams, and J. B. Gill (1998a), Investigating solid mantle upwelling rates beneath mid-ocean ridges using U-series disequilibria, 1: A global approach, *Earth Planet. Sci. Lett.*, *157*, 151–165.

Lundstrom, C. C., Q. Williams, and J. B. Gill (1998b), Investigating solid mantle upwelling rates beneath mid-ocean ridges using U-series disequilibria, II. A local study at 33°S Mid-Atlantic Ridge, *Earth Planet. Sci. Lett.*, *157*, 167–181.

Lundstrom, C. C., D. E. Sampson, M. R. Perfit, J. Gill, and Q. Williams (1999), Insights into mid-ocean ridge basalt petrogenesis: U-series disequilibria from the Siqueiros Transform, Lamont Seamounts, and East Pacific rise, *J. Geophys. Res.*, *104*, 13,035–13,048.

Marty, B. (1995), Nitrogen content of the mantle inferred from N_2-Ar correlation in oceanic basalts, *Nature*, *377*, 326–329.

Marty, B., and I. Tolstikhin (1998), CO_2 fluxes from mid-ocean ridges, arc and plumes, *Chem. Geol.*, *145*, 233–248.

McCulloch, M. T., and V. C. Bennett (1994), Progressive growth of the Earth's continental crust and depleted mantle: Geochemical constraints, *Geochim. Cosmochim. Acta*, *58*, 4717–4738.

McDonough, W. F., and S.-S. Sun (1995), The composition of the Earth, *Chem. Geol.*, *120*, 223–253.

Meisel, T., R. J. Walker, and J. W. Morgan (1996), The osmium isotopic composition of the Earth's primitive upper mantle, *Nature*, *383*, 517–520.

Michael, P. (1995), Regionally distinctive sources of depleted MORB: Evidence from trace elements and H_2O, *Earth Planet. Sci. Lett.*, *131*, 301–320.

Moreira, M., and C. J. Allègre (1998), Helium-neon systematics and the structure of the mantle, *Chem. Geol.*, *147*, 53–59.

Morgan, J. W., G. A. Wandless, R. K. Petrie, and A. J. Irving (1981), Composition of the Earth's upper mantle-I. Siderophile trace elements in ultramafic nodules, *Tectonophysics*, *75*, 47–67.

Mortlock, R. A., and P. N. Froelich (1987), Continental weathering of germanium: Ge/Si in the global river discharge, *Geochim. Cosmochim. Acta*, *51*(8), 2075–2082.

Newsom, H. E., W. M. White, K. P. Jochum, and A. W. Hofmann (1986), Siderophile and chalcophile element abundances in oceanic basalts, Pb isotope evolution and growth of the Earth's core, *Earth Planet. Sci. Lett.*, *80*, 299–313.

Patchett, P. J., J. D. Vervoort, U. Söderlund, and V. J. M. Salters (2004), Lu-Hf and Sm-Nd isotopic systematics in chondrites and their constraints on the Lu-Hf properties of the Earth, *Earth Planet. Sci. Lett*, in press.

Pattou, L., J. P. Lorand, and M. Gros (1996), Non-chondritic platinum group element ratios in the Earth's mantle, *Nature*, *379*, 712–715.

Paul, D., W. M. White, and D. L. Turcotte (2002), Modelling the isotopic evolution of the Earth, *Philos. Trans. R. Soc. London, Ser. A*, *360*, 2433–2474.

Rudnick, R. L., and S. Gao (2003), The composition of the continental crust, in *The Crust*, vol. 3, edited by R. L. Rudnick, pp. 1–64, Elsevier Sci., New York.

Ryan, J. G., and C. H. Langmuir (1987), The systematics of lithium abundances in young volcanic rocks, *Geochim. Cosmochim. Acta*, *51*, 1727–1741.

Ryan, J. G., and C. H. Langmuir (1993), The systematics of boron abundances in young volcanic rocks, *Geochim. Cosmochim. Acta*, *57*, 1489–1498.

Saal, A., E. H. Hauri, C. H. Langmuir, and M. R. Perfit (2002), Vapor undersaturation in primitive mid-ocean ridge basalt and the volatile content of the Earth's upper mantle, *Nature*, *419*, 451–455.

Salters, V. J. M. (1996), The generation of mid-ocean ridge basalts from the Hf and Nd isotope perspective, *Earth Planet. Sci. Lett.*, *141*, 109–123.

Salters, V. J. M., and H. J. B. Dick (2002), Mineralogy of the mid-ocean ridge basalt source from neodymium isotopic composition in abyssal peridotites, *Nature*, *418*, 68–72.

Salters, V. J. M., and S. R. Hart (1989), The Hf-paradox, and the role of garnet in the MORB source, *Nature*, *342*, 420–422.

Salters, V. J. M., and J. E. Longhi (1999), Trace element partitioning during the initial stages of melting beneath ocean ridges, *Earth Planet. Sci. Lett.*, *166*, 15–30.

Salters, V. J. M., J. E. Longhi, and M. Bizimis (2002), Near mantle solidus trace element partitioning at pressures up to 3.4 GPa, *Geochem. Geophys. Geosyst.*, *3*(7), 1038, doi:10.1029/2001GC000148.

Sarda, P., and D. Graham (1990), Mid-ocean ridge popping rocks: Implications for degassing at ridge crests, *Earth Planet. Sci. Lett.*, *97*, 268–289.

Scherer, E., C. Münker, and K. Mezger (2001), Calibrating the Lu-Hf clock, *Science*, *293*, 683–686.

Schiano, P., J. Birck, and C. J. Allègre (1997), Osmium-strontium-neodymium-lead isotopic covariations in mid-ocean ridge basalt glasses and the heterogeneity of the upper mantle, *Earth Planet. Sci. Lett.*, *150*, 363–379.

Schilling, J.-G. (1975), Rare-earth variations across "normal segments" of the Reykjanes Ridge, 60°–53°N, Mid-Atlantic Ridge, 29°S, and East Pacific Rise, 2°–19°S, and evidence on the composition of the underlying low-velocity layer, *J. Geophys. Res.*, *80*(11), 1459–1473.

Shirey, S. B., and R. J. Walker (1998), The Re-Os system in cosmochemistry and high-temperature geochemistry, *Annu. Rev. Earth Planet. Sci.*, *26*, 423–500.

Sims, K. W. W., H. E. Newsom, and E. S. Gladney (1990), Chemical fractionation during formation of the Earth's core and continental crust: Clues from As, Sb, W and Mo, in *Origin of Earth*, edited by H. E. Newsom and J. H. Jones, pp. 291–317, Oxford Univ. Press, New York.

Sims, K. W. W., et al. (2002), Chemical and isotopic constraints on the generation and transport of magma beneath the East Pacific Rise, *Geochim. Cosmochim. Acta*, *66*, 3481–3504.

Snow, J. E., and L. Reisberg (1995), Os isotopic systematics of the MORB mantle: Results from altered abyssal peridotites, *Earth Planet. Sci. Lett.*, *136*(3–4), 723–733.

Snow, J. E., and G. Schmidt (1998), Constraints on Earth accretion deduced from noble metals in the oceanic mantle, *Nature*, *391*(6663), 166–169.

Snow, J. E., G. Schmidt, and E. Rampone (2000), Os isotopes and highly siderophile elements (HSE) in the Ligurian ophiolites, Italy, *Earth Planet. Sci. Lett.*, *175*(1–2), 119–132.

Söderlund, U., P. J. Patchett, J. D. Vervoort, and C. E. Isachsen (2004), The 176Lu constant determined by Lu-Hf and U-Pb isotope systematics of Precambrian mafic intrusions, *Earth Planet. Sci. Lett.*, *219*, 311–324.

Stracke, A., M. Bizimis, and V. J. M. Salters (2003a), Recycling oceanic crust: Quantitative constraints, *Geochem. Geophys. Geosyst.*, *4*(3), 8003, doi:10.1029/2001GC000223.

Stracke, A., A. Zindler, V. J. M. Salters, D. McKenzie, J. Blichert-Toft, F. Albarède, and K. Grönvold (2003b), Theistareykir revisited, *Geochem. Geophys. Geosyst.*, *4*(2), 8507, doi:10.1029/2001GC000201.

Stracke, A., A. Zindler, V. J. M. Salters, D. McKenzie, and K. Grönvold (2003c), The dynamics of melting beneath Theistareykir, northern Iceland, *Geochem. Geophys. Geosyst.*, *4*(10), 8513, doi:10.1029/2002GC000347.

Sun, S.-S. (1982), Chemical composition and origin of the Earth's primitive mantle, *Geochim. Cosmochim. Acta*, *46*, 179–192.

Sun, S.-S., and W. F. McDonough (1989), Chemical and isotopic systematics of oceanic basalts: Implications for mantle composition and processes, in *Magmatism in the Ocean Basins*, edited by A. D. Saunders and M. J. Norry, *Geol. Soc. Spec. Publ.*, *42*, 313–345.

Sun, W., V. C. Bennett, S. M. Eggins, R. J. Arculus, and M. R. Perfit (2003), Rhenium systematics in submarine MORB and back-arc basin glasses: Laser ablation ICP-MS results, *Chem. Geol.*, *196*, 259–281.

Tatsumoto, M. (1978), Isotopic composition of lead in oceanic basalts and its implication to mantle evolution, *Earth Planet. Sci. Lett.*, *38*, 63–87.

Tatsumoto, M., D. M. Unruh, P. Stille, and H. Fujimaki (1984), Pb, Sr, and Nd isotopes in Oceanic Island basalts, in *Proceedings of the 27th International Geological Congress, Geochemistry and Cosmochemistry*, pp. 485–501, VNU Sci. Press, Zeist, Netherlands.

Turcotte, D. L., D. Paul, and W. M. White (2001), Thorium-uranium systematics require layered mantle convection, *J. Geophys. Res.*, *106*, 4265–4276.

Wendt, J. I., M. Regelous, Y. Niu, R. Hékinian, and K. D. Collerson (1999), Geochemistry of lavas from the Garrett Transform Fault: Insights into mantle heterogeneity beneath the eastern Pacific, *Earth Planet. Sci. Lett.*, *173*, 271–284.

White, R. S., D. McKenzie, and A. K. O'Nions (1992), Oceanic crustal thickness from seismic measurements and rare earth element inversions, *J. Geophys. Res.*, *97*, 19,683–19,715.

White, W. M. (1993), ^{238}U/^{204}Pb in MORB and open system evolution of the depleted mantle, *Earth Planet. Sci. Lett.*, *115*, 211–226.

Yi, W., A. N. Halliday, J. C. Alt, D. C. Lee, M. Rehkamper, M. O. Garcia, and Y. J. Su (2000), Cadmium, indium, tin, tellurium, and sulfur in oceanic basalts: Implications for chalcophile element fractionation in the Earth, *J. Geophys. Res.*, *105*(B8), 18,927–18,948.

Yin, Q., S. B. Jacobsen, K. Yamashita, J. Blichert-Toft, P. Télouk, and F. Albarède (2002), A short timescale for terrestrial planet formation from Hf-W chronometry of meteorites, *Nature*, *418*, 949–952.

Zindler, A., and S. R. Hart (1986), Chemical geodynamics, *Annu. Rev. Earth Planet. Sci.*, *14*, 493–571.

Zindler, A., and E. Jagoutz (1988), Mantle cryptology, *Geochim. Cosmochim. Acta*, *52*, 319–333.

Zindler, A., H. Staudigel, and R. Batizza (1984), Isotope and trace element geochemistry of young Pacific seamounts: Implications for the scale of upper mantle heterogeneity, *Earth Planet. Sci. Lett.*, *70*, 175–195.